Review Article

Yapeng Wang, Zhaofeng Chen*, Yeshang Lu, Lixia Yang*, Ting Xu, Haisheng Wu, Jianxun Zhang, and Lihua He

A review of application, modification, and prospect of melamine foam

https://doi.org/10.1515/ntrev-2023-0137
received February 22, 2023; accepted September 24, 2023

Abstract: Melamine foam (MF), a promising development in light materials, finds application in construction, agriculture, aviation, transportation, electronic message, and other fields due to its excellent thermal insulation performance, sound absorption and noise reduction capabilities, safety and health benefits, as well as easy processing. However, its own shortcomings such as hardness, poor toughness, fragility, and slag removal greatly limit its application scope. In this review, a survey of the literature from two aspects of toughening of melamine resin and regulation of MF pore structure are reviewed to explore the research progress of toughening modification of MF. The principle, merit, and demerit of different modification methods are analyzed. In addition, owing to the extensive literature available, this article also summarizes the representative achievements of the nanotechnology modification of MF derivatives (carbon foam and carbon aerogel). Eventually, based on an assessment of current application status for both MF and its derivatives while considering existing challenges in their modification processes using nanotechnology approaches, we discuss future prospects for their application.

Keywords: melamine foam, melamine resin, nanotechnology modification, carbon foam, carbon aerogel

*** Corresponding author: Zhaofeng Chen**, School of Material Science and Technology, Nanjing University of Aeronautics and Astronautics, Nanjing, 211106, China, e-mail: zhaofeng_chen@163.com
*** Corresponding author: Lixia Yang**, School of Material Science and Technology, Nanjing University of Aeronautics and Astronautics, Nanjing, 211106, China, e-mail: lixiayang@nuaa.edu.cn
Yapeng Wang, Yeshang Lu: School of Material Science and Technology, Nanjing University of Aeronautics and Astronautics, Nanjing, 211106, China
Ting Xu, Haisheng Wu: Beijing spacecrafts Co., Ltd, Beijing, 100048, China
Jianxun Zhang, Lihua He: Puyang Greencos New Material Technology Co., Ltd, Puyang, 457000, China

1 Introduction

Melamine foam (MF) is an inherently flame-retardant foam derived from melamine formaldehyde resin by curing and foaming process [1]. In addition to its excellent flame-retardant property [2], it also exhibits good sound absorption [3], low density [4], high porosity [5], heat resistance, and preservation [6]. Consequently, MF finds applications in the development of oil–water separation materials [7,8], supercapacitors [9,10], sound absorption materials [11,12], vacuum insulated panels [13], *etc*. The performance characteristics and service range of MF are shown in Table 1. At present, domestic enterprises have made great progress in the development and application of MF, such as Puyang Greencos New Material Technology Co., Ltd, whose MF products have important application value in civil, industrial, construction, transportation, aviation, military, and other fields (Figure 1) [14–16].

1.1 Sound-absorbing application of MF

The MF possesses a fully open three-dimensional mesh structure (Figure 2), with a length to diameter ratio (L/D) of the mesh ranging from approximately 10–20. Its high opening rate characteristics (≥99%) enable sound waves to effectively penetrate the deep layer of the foam body, where they are rapidly dissipated through vibration of the MF gridding. As a result, reflected sound waves are effectively eliminated, leading to enhanced sound absorption performance [12,29]. Due to its excellent sound-absorbing performance, MF has been successfully applied to the sound absorbing materials for military and civilian use [30].

Yang *et al*. [31] investigated the sound insulation of phenolic resin modified MF. The experimental results illustrated that the sound insulation property of MF modified by phenolic resin was remarkably improved compared to that without phenolic resin. Li *et al*. [32] developed a thin and lightweight sound absorber by utilizing MF's excellent sound absorption performance. The research results showed

Table 1: Performance characteristics and service range of MF

Project	Performance	Service scope	Reference
Density	Low (<8 kg/m^3)	oil–water separation material and building, *etc.*	[17–20]
Sound insulation	Excellent	Rail vehicles, aircrafts cabin, and automobile, *etc.*	[3,21–23]
Opening rate	High (99%)	oil–water separation material and EMI shielding, wastewater purification, *etc.*	[24–26]
Heat insulation	Eminent	Building and vacuum insulated panels, *etc.*	[27,28]

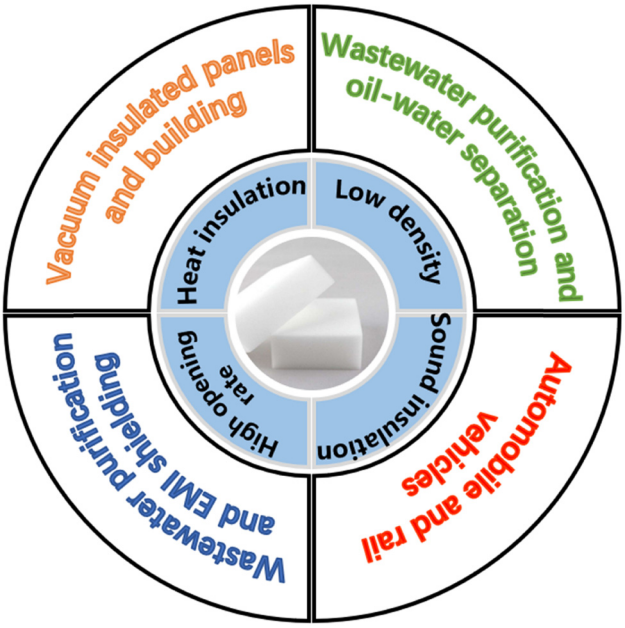

Figure 1: Typical applications of MF prepared by Puyang Greencos New Material Technology Co., Ltd.

that incorporating a hollow perforated spherical structure with MF maintained effective sound absorption within the frequency range of 200–1,600 Hz, despite limited thickness constraints. These results also suggested that the proposed absorbers have great potential for use in noise control applications.

To investigate the sound absorption performance of MF and cotton, Li *et al.* [33] established a scaled down cylindrical section noise experimental device according to the objective conditions of the experiment and the application range of the simulation software. The experiment results showed that the noise reduction effect of MF with the same quality is about 1.42 times more than that of sound-absorbing cotton. In addition, MF can also be used as sound insulation panels of sports venues, lining of roll gate boxes, sound insulation materials of impellers of air conditioning and ventilation equipment, inner lining of fan hoods, *etc.* [34,35].

1.2 Oil–water separation application of MF

MF is characterized by high porosity, large surface area, low density, and low cost [4]. The inside of MF is composed of a large number of spheroid units, whose surface is a three-dimensional network skeleton ring of pentagon structure, which makes the surface water film tension of MF high after water absorption, so it has a strong water absorption ability [19,23]. Consequently, when hydrophobically modified, the high surface area enables fast oil absorption by MF and makes it an ideal material for oil–water separation applications [16,36].

Duan *et al.* [5] reported a simple method to prepare high-performance oil absorbents by loading ball-mill

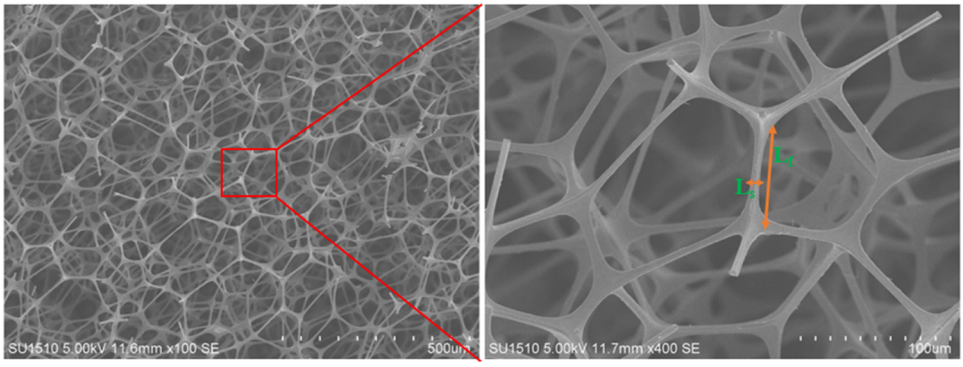

Figure 2: Microscopic characterization of MF.

biochar (BMBC) and octadecylamine onto MF skeleton. The experimental results showed that BMBC successfully transformed the hydrophilic surface of MF into a hydrophobic surface, and endowed MF with higher oil absorption capacity (43–155 times dead weight) and excellent recyclability. Mu *et al.* [37] presented a superhydrophobic foam *via* coating the hydrolyzed alkylsilane on the skeleton of commercial MF. The study results (Figure 3) showed that the wettability of MF changed to superhydrophobic due to the presence of alkylsilane, which exhibited excellent oil absorption capacity and exceptional recyclability. Moreover, the modified MF could be readily used in industrial oil spill clean-up.

oil–water separation modification generally requires polymers with low surface energy (such as polysiloxane, fluoropolymer, or long alkyl) to cover the surface of melamine sponge through a series of reactions [38,39], or high temperature pyrolysis to remove the hydrophilic groups on the surface of melamine sponge to improve its hydrophobicity [36]. After hydrophobic modification, MF can absorb leaked oil or organic solvent.

1.3 Heat insulation application of MF

There are a lot of studies, which showed that MF has a high cross-linked three-dimensional network structure system to keep excellent thermal stability and aging resistance [40,41]. The research results show that MF starts to burn only when the surface is in contact with an open flame. Once the combustion starts, the decompositions immediately produce a large amount of inert non-flammable gas, which slows down the combustion rate. At the same time, a dense coke layer is formed quickly on the surface of the burner, which effectively blocks the development of combustion to the deep layer, and automatically extinguishes after the open flame leaves [42,43]. MF can work at 200°C for a long time, without decomposition and deformation, and obvious decomposition only appears when the temperature increases above 350°C [13,43]. While for other forms, such as polyvinyl chloride, polyolefin, polystyrene, and polyurethane (PU), deformation and decomposition occur when the working temperature exceeds 120°C. The resistance to open flame ignition experiment of MF and the maximum temperature for long service time of some forms are shown in Figure 4.

Based on the exceptional flame retardant and heat insulation properties, MF exhibits significant potential for application in constructing energy conservation buildings and vacuum insulation panel (VIP) [13,47,48]. Li *et al.* [49] utilized a MF prepolymer derived from melamine and paraformaldehyde as the matrix material, cyclohexane as the foaming agent, dimethicone as the foam stabilizer, and hydrochloric acid as the catalyst. The MF rigid foam with high closed-cell content was prepared using an oven heating method. The prepared MF foams demonstrated great comprehensive performance with closed cell content of 83.5%, water absorption of 12.0%, compressive strength of 292 kPa, thermal conductivity of 0.033 W/(m K) and limiting oxygen index (LOI) of 36%. Compared to conventional organic foams, the as-prepared MF

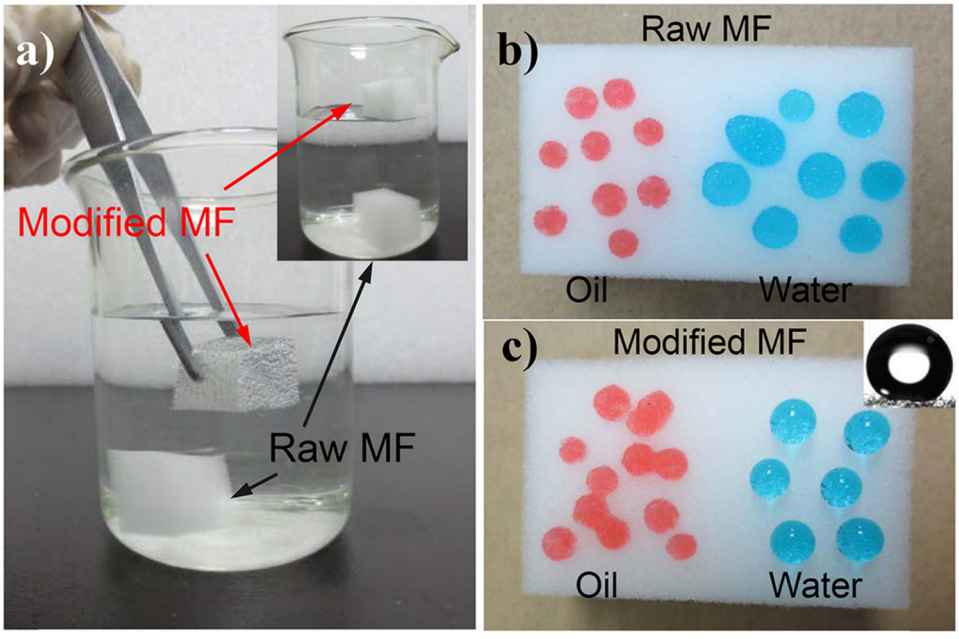

Figure 3: Hydrophobic and oleophilic properties of (a) MF, (b) before treatment, and (C) after treatment [37].

Project	Maximum temperature for long service (°C)
MF	200
polyolefin	100
polystyrene	60
polyurethane	120
polyvinyl chloride	60

Figure 4: The resistance to open flame ignition experiment of MF and the maximum temperature for long service of some forms [13,44–46].

foams can be used as thermal insulation material for building exterior walls. Kavsek *et al.* [50] used pentane to blow melamine-formaldehyde resin emulsion and further catalyze and heat cure to prepare a new melamine-formaldehyde rigid foam material. Compared with other organic polymer foams, the produced MF foam has the characteristics of superior fire resistance, chemical stability, and low density, which made MF foam potentially useful in the manufacture of VIPs.

1.4 Preparation process and disadvantages of MF

1.4.1 The preparation process of MF

The preparation of MF is usually divided into two processes: resin synthesis and curing foaming (Figure 5) [13,51]. The synthesis stage of melamine resin (MR) can be divided into two steps. First, the melamine and formaldehyde are dissolved in a weakly alkaline medium (pH = 8.5–9.0). Because melamine and formaldehyde will produce insoluble methylene melamine precipitation under acidic conditions, it is necessary to adjust the pH value of the solvent between 8.5 and 9.0 before the reaction, so as to ensure that the pH value of the reaction process is between 7.0 and 7.5. When the external temperature is in the range of 80–90°C, melamine and formaldehyde take place addition reaction to form hydroxymethyl melamine. Second, hydroxymethyl melamine is further poly-condensed in neutral or weakly alkaline media, resulting in low molecular polymer (MR) linked by dimethylene ether bond or methylene bond [52–54]. The reaction mechanism of MR is shown in Figure 6 [37]. The curing foaming process is to mix MR with emulsifier, curing agent, and foaming agent adequately and then the cross-linking

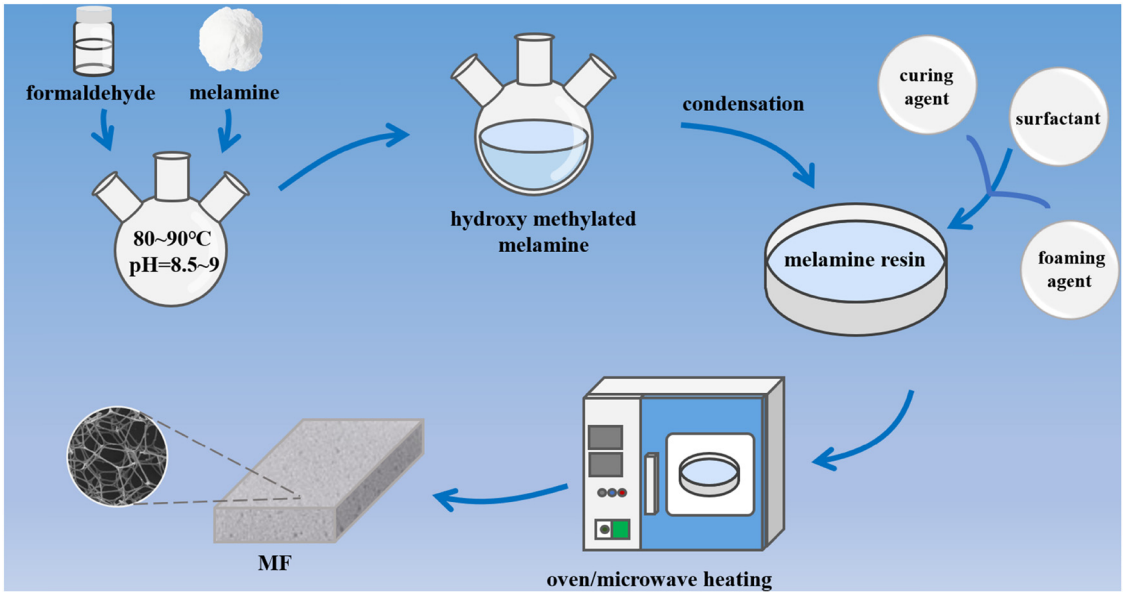

Figure 5: The production process of MFs.

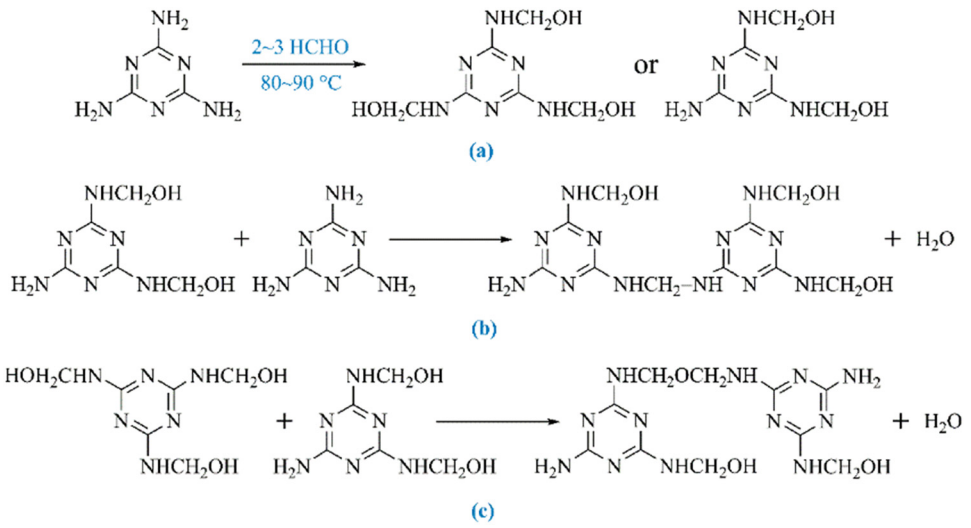

Figure 6: The reaction mechanism of MR [13,51]. (a) Formation of methylol melamine. (b) Condensation of methylol of methylol melamine and amino of melamine. (c) Condensation of methylol of methylol melamine and one another.

reaction occurs by microwave or oven heating to form polymer foam with three-dimensional network structure (MF) [55].

1.4.2 Disadvantages and toughening modification prospect of MF

Although MF possesses high porosity, low density, high opening rate, and good flame retardancy, its inherent drawbacks such as hardness, poor toughness, fragility, and slag removal significantly limit its application scope [16]. The infrared spectrum of MF is shown in Figure 7. The wave numbers of 808, 1,331, 1,478, and 1,549 cm^{-1} correspond to the in-plane deformation of the triazine ring and the contraction and torsion of C═N in the triazine ring [56]. It is well known that the reason for the high brittleness of MF is that its molecular structure contains a large number of rigid triazine rings and the flexible carbon chains between them are short [57]. Consequently, enhancing the toughness of MF has become a prominent research topic in recent years.

At present, most scholars have only explored the methods of toughening, strengthening, and improving the dimensional stability of MF; however, few experts have comprehensively summarized the causes of poor toughness and modified toughening methods. Generally speaking, the toughness of MF depends on both the properties of MR and foam microstructure. In this study, the methods of toughening modification of MF are described in detail from two aspects of toughening modification of MR and microstructure regulation of foam. Furthermore, the direction of

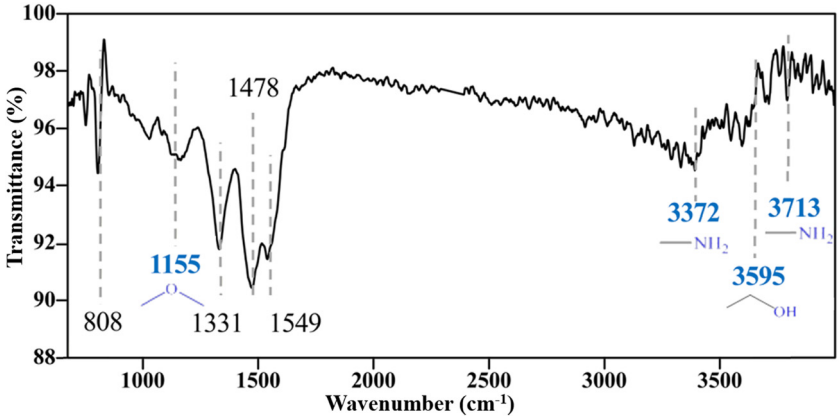

Figure 7: The infrared spectrum of MF [56].

toughening modification methods, and the application of MF products and their derivatives in the future are prospected.

2 Modification of MR

MR is a type of thermosetting resin wherein the properties are determined by the degree of curing [58]. The MR solution needs to be heated and cured in the process of use, so that the oligomers are gradually cross-linked to form a polymer with a three-dimensional network structure. If the MR is not cured completely, its adhesion, water resistance, chemical corrosion resistance, and other properties will be reduced [59]. The curing of MR is achieved by cross-linking methylene or dimethylene ether bonds, and its molecular structure is shown in Figure 8. At present, the toughening modification of MR mainly includes physical modification, flexible chain lengthening, and functional group end sealing [12,60,61]. The section will focus on these three approaches.

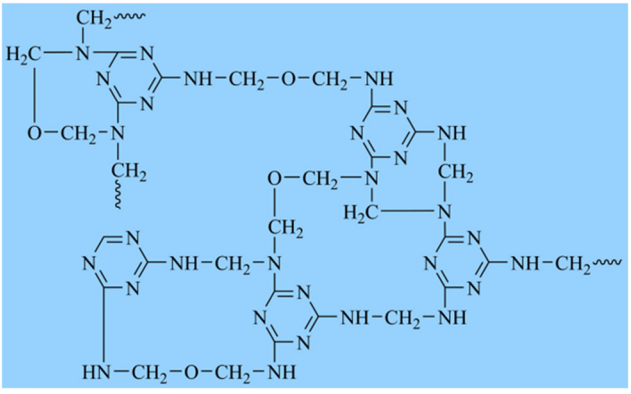

Figure 8: Molecular structure of MR [12,60,61].

2.1 Physical modification of MR modification

In the physical modification method, the modifier is combined with MR by blending method to prevent the triazine rings from getting close to each other, so as to realize the toughening of MR. The common physical modifiers mainly include nanoparticles, flexible polymers, and fiber materials [62–66].

2.1.1 Modification by adding nanoparticles

The addition of nanoparticles is a widely used approach to modify MR [67–70]. Nanoparticles have the characteristics of large specific surface area, a large number of unsaturated bonds on the surface, small size, and high surface activity [71,72]. When adding a small number of nanoparticles, the surface functional groups of MR react with these nanoparticles to generate an interfacial force that surpasses the van der Waals force. When the MR is subjected to external force, the nanoparticles can absorb part of the impact energy, so as to realize the toughening of the MR [63].

Based on the source, type, size, content, and shape, nanoparticles can reinforce various properties of the substrate MR (as summarized in Table 2). Therefore, nanomaterials can affect MR nanocomposites' final properties such as mechanical properties, curing behavior, formaldehyde emission, and flame retardancy even at low addition levels [15]. Commonly employed nanofillers include clay minerals, different oxides, carbon-based nanomaterials, graphite, cellulose nano-fiber, metals and metal alloys, *etc.* [61,73].

For instance, Li *et al.* [61] demonstrated that the incorporation of a dispersed peg-nano SiO_2 solution into the melamine/formaldehyde mixture could enhance the physical properties (such as curing time, free formaldehyde content, and elongation at break) of MR. The experimental

Table 2: Nanomaterials and their enhanced performance of MR

Type of nanomaterials		Performance (enhanced)	References
Mineral nanoparticles	Montmorillonite	Thermal stability, chemical resistance, processability	[74,75]
	Clay	Thermal stability, low cost, mechanical, *etc.*	[76,77]
Bio-based additive	Cellulose nanocrystals	Mechanical strength, *etc.*	[78,79]
	Carbon nanotubes	Heat insulation performance, *etc.*	[80,81]
Metal-based nanoparticles	Fe	Fouling resistance, good wettability, *etc.*	[82]
	Ni	Specific capacitance value, *etc.*	[83]
Oxides nanoparticles	SiO_2	Thermal stability, toughness, flame-retardant properties, impact strength, *etc.*	[84–86]
	TiO_2	Thermal stability, smoke suppression, *etc.*	[87,88]

findings suggested that the addition of dispersed nano-SiO_2 has the potential to improve toughness and other desirable characteristics in modified MR. However, excessive nanoparticle loading may result in uneven dispersion and agglomeration, thereby compromising its toughening effect.

2.1.2 Modification by flexible short chain polymers and fiber materials

Adding flexible short chain polymers and fiber material such as starch, carbon fiber (CF) [64], polyvinyl alcohol (PVA) [89,90], and PU [91] to MR is another common physical modification method. These modifiers contain numerous polar groups that can form hydrogen bonds or covalent bonds with MR to enhance its toughness. Lulu *et al.* [92] studied the effect of PVA on the properties of MR. The results showed that the blending fiber was endowed with effective flame- retardant property by the amino group and triazine ring group in melamine/PVA fibers, and the LOI reached 28–31. The best homogeneity of blended fibers was achieved when the solid content ratio between MR and PVA blend was 1:1. PVA could effectively improve the crystallinity, mechanical properties, and elasticity of MR.

Li *et al.* [64] prepared melamine-formaldehyde rigid closed-cell foams that were toughened by ethylene glycol (EG) and CF. Compared to unmodified MF rigid foams, these tough rigid closed-cell MF exhibited excellent pulverization rate, compressive strength, bending strength, cellular structure integrity, thermal insulation performance as well as flame resistance characteristics. It is worth mentioning that when the fiber is used as toughening agent, the viscosity of the resin will increase, and the mixing effect of the foaming agent will become worse in the foaming process, thus affecting the final performance of the foam. Fiber materials have been gradually phased out as toughening agents.

2.1.3 Summary of physical modification of MR

As a whole, when nanoparticles are added as modifiers, too much nanoparticles will result in agglomeration, and too little nanoparticles will limit the toughening modification effect, the solutions improve the dispersion and compatibility of nanoparticles by modifying nanoparticles in resin [93]. The modification of MR by adding flexible long chain polymer is another common physical modification method. The polar groups on the surface of flexible long chain polymer can form hydrogen bonds and covalent bonds with the surface of MR, so as to achieve the toughening effect [94,95]. Moreover, the use of fiber material as toughening agent may affect the foaming effect of resin, which has been gradually eliminated [96]. The toughening by physical modification has the characteristics of simple, effective, and economical and practical, and has broad development space.

2.2 Functional group end-sealing method of MR modification

The functional group end-sealing method involves the reaction of modifying agents with melamine or hydroxymethyl melamine, resulting in the shielding of one amino group on the triazine ring to reduce cross-linking density. Small molecules with single functional groups, such as methanol, ethanol, aniline, and p-toluene sulfonamide, are often used as functional group shielding modifiers [65]. Fei *et al.* [97] prepared fragrance microcapsules by *in situ* polymerization of methanol-modified melamine-formaldehyde resin. FT-IR results showed that the essential oil was encapsulated by MR, and TG-DTG test showed that micro-encapsulation significantly improved the thermal stability of MR.

Furthermore, derivatives of melamine such as benzene melamine, aromatic melamine, and alkyl substituted melamine are also often used as modifiers. It is worth noting that the synthetic conditions of melamine derivatives are relatively complex and the yield is not high, so they cannot be commercialized on a large scale and are usually used in high-end markets such as aerospace. Therefore, the economical and suitable modifiers need to be further studied.

2.3 Flexible chain lengthening of MR modification

The high brittleness of MF is attributed to its molecular structure, which contains a large number of rigid triazine rings and short flexible carbon chains between them (as mentioned in Figure 5) [57]. Therefore, flexible chain lengthening is put forward to improve the flexibility of MR by increasing the length of the flexible chain between the triazine rings. Modifiers generally contain a variety of functional groups that can react with hydroxyl methyl groups or amino groups, and the distances between triazine rings are increased by molecular bonding. The flexible chain lengthening method is a common chemical modification idea. The flexible chain lengthening method makes the

molecular chains of MR have greater intramolecular deformability than that of methylene linkage, and reduces the crosslinking density of resin, so as to improve the flexibility of MF. PVA and allyl glycidyl ether are often used as multi-functional small molecule modifiers to increase the flexible chain length between the triazine rings [66].

Chen *et al.* [98] used PVA and benzoguanamine to modify MF resin, while investigating the enhanced tensile strength and flame retardant properties of the modified MR. Compared with the unmodified MR, the tensile strength and flame retardancy properties of the modified MR were improved. Yan *et al.* [12] employed allyl glycidyl ether to modify MR, and the modified resin was able to demonstrate a longer storage duration as compared to the conventional resins, and the storage time for the modified resin exceeded 90 days, and the free formaldehyde content was lower than 0.05 ppm. Additionally, the as-prepared foam exhibited excellent flame retardancy properties, low-volume water absorption, and lower thermal conductivity. Concurrently, the foam prepared based on the optimal conditions possessed a high compressive strength of 5.08 MPa, which was 17.5 times higher than that of the conventional MF. But, allyl glycidyl ether itself is toxic, so its application on MR is limited. The comparison of the performance of MF modified by allyl glycidyl ether and other previous studies are illustrated in Table 3.

In conclusion, both long-chain polymers and small-molecule compounds can improve the flexibility of MR by increasing the flexible chain length, and affect the heat resistance or flame retardancy of MR. However, common modifiers process toxicity, so this method is limited to incorporating modifications. Therefore, in order to effectively enhance the toughness of MF, molecular structure design should be prioritized.

2.4 A comprehensive analysis of MR modification methods

Overall, the three toughening modification methods of MR showed that physical modification can block the proximity of triazine rings; flexible chain lengthening and functional group end-sealing method can change the molecular structure of the resin. All these modification techniques contribute to a reduction in crosslink density of MR; however, their individual toughening effects are limited. For instance, Li *et al.* [61] used polyethylene glycol (PEG) to modify nano-SiO_2 particles, and uniformly dispersed the modified solution into the melamine/formaldehyde mixture, thereby, the curing time and elongation at break of the MR were improved (Table 4). The addition of 0.42% PEG-modified SiO_2 reduced the glass transition temperature of the MR by 29.4°C, and thermogravimetric (TG) spectroscopy showed that the introduction of nano-SiO_2 into the MR hardly affected its thermal stability. These results also indicated that the addition of PEG-modified nano- SiO_2 can improve the elongation at break of MR. Therefore, further investigation is required to explore synergistic toughening approaches using a combination of different methods while ensuring flame retardancy and mechanical properties consistent with MF.

3 Regulation of MF pore structure

The pore structure directly affects the physical properties of MF [62]. During the foaming process, bubbles are generated and expanded, while the prepolymer gradually

Table 4: Effect of nano silica addition on the physical properties of MR [61]

Amount of nano silica (%)	Cure time (s)	Elongation at break (%)
0	109 ± 3	5.35 ± 1.52
0.3	94 ± 2	16.20 ± 2.61
0.36	93 ± 4	13.00 ± 2.13
0.42	95 ± 1	19.90 ± 2.86
0.48	94 ± 2	9.45 ± 2.01

Table 3: Comparison of the performance of MF modified by allyl glycidyl ether and other studies [12]

Project	Traditional MF	CF/EG	Dimethicone	MF modified by allyl glycidyl ether
Apparent density (g/cm^3)	0.040	0.078	0.063	0.250
Thermal conductivity (W/m K)	0.030	0.031	0.033	0.0256
Compressive strength (MPa)	0.23	0.44	0.292	5.08
Volumetric water absorption (%)	1.4	9.0	10	0.9
LOI (%)	39.4	39.6	39	38.9

undergoes cross-linking to increase viscosity. In the later stage, the large foam bursts or even connects to form the open-cell foam. If it does not burst, it is the closed-cell foam [36]. The final pore structure of MF is controlled by two processes: foaming and curing. The curing rate of the resin primarily depends on the viscosity of the resin, solid content, curing agent dosage, *etc*., whereas the foaming rate is mainly determined by foaming agent, foaming method, and foaming process [1,12,19]. Therefore, investigating how these factors affect both mechanical properties and microstructure of foam is crucial for enhancing the toughening effect of MF.

3.1 Physical properties of MR solution

The viscosity of MR solutions is a crucial factor that affects its foaming properties [49,99]. Zhang *et al*. [100] prepared open and closed cell thermosetting foams using MR and formaldehyde as the main raw materials, and investigated the impact of prepolymer viscosity on foam density and structure. The results showed that low initial viscosity resulted in open-cell foam formation while increasing viscosity led to incomplete bubble expansion resulting in closed-cell foam production. For open-cell foam (Figure 9), low viscosity solution resulted in bubble growth instability and collapse, and the bubble forming rate was low, which resulted in high density. With the increase in viscosity, the bubble forming rate increased and the density decreased. When the density increased again, the pores became smaller and denser, the density and the toughness increased again. For closed-cell foam, the higher the viscosity, the smaller the bubble hole and the higher the foam density (Figure 10). In both cases, there was an optimal viscosity that minimized the foam density formed, about 70 mPa s for the open-cell foams and 850 mPa s for the closed-cell foams. Moreover, only within this appropriate range did MF foam exhibit uniform bubble holes resulting in good toughness.

On the other hand, the solid content of MR is another one of the important factors affecting its foaming. Ruipeng *et al*. [101] analyzed the effect of solid content of MR on the physical properties and mechanical properties of MF. The results showed that when the solid content was too low, shrinkage bubble phenomenon occurred, but when the solid content increased, the reaction system and resin storage stability became worse, and more strict process control was needed. In addition, when the solid content of melamine formaldehyde resin was 69%, the flexural strength of MF reached the best, *i.e*., 305 kPa.

3.2 Foaming method

The foaming methods of MF mainly include oven foaming and microwave foaming [49,64]. Xia and Wang [29,62] reported and compared the microstructure of MF prepared by these two methods. As shown in Figure 11a, the bubble hole formed during oven foaming exhibited a predominantly open-hole through structure resembling rigid spheres with approximately 14–16 sides. Due to the thickness of the foam wall, most of the skeletons were piled together and showed a sheet shape. The aspect ratio (H/D) of the foam was between 1 and 2, so the flexibility was poor and the rigidity was strong. In contrast, as shown in Figure 11b, microwave-induced MF primarily consisted of interconnected ligamentous skeletons that were linked *via* three-tip inner swing tops, thereby increasing contact area and enhancing stability. Moreover, the length-to-diameter ratio (L/D value) of this mesh-like structure reached approximately 15, leading to improved toughness. This can be attributed mainly to the faster heating rate associated with microwave processing compared to oven foaming; uniform heating without temperature gradients allowed for instantaneous boiling and bubbling of the foaming agent, thus yielding a more pronounced three-dimensional network skeleton structure.

In fact, the length to diameter ratio and framework of MF formed by microwave and oven were very different, resulting in significant differences in the mechanical properties of MF. When applying pressure to the moicrowave-foamed MF frame by microwave, the frame can produce significant bending and torsion deformation, and the bending and torsion deformation back quickly when the external force removed. Macroscopically, the compression test showed the bending deformation between layers, and the local structural failure was inhibited by the contact generated by the bending deformation between skeletons. Hence, the damage spreading trend was avoided and showed good flexibility [102,103]. However, when the MF foamed by oven was stressed, the rigid skeleton did not undergo bending deformation when the load was transferred between adjacent layers, and the load continued to penetrate into the middle of the next layer of foam body, which resulted in cracks and bubble burst [29,62].

In addition, microwave penetration ensured even heating throughout the foam body; once microwaves ceased heating, the temperature inside returned to room temperature rapidly. Microwave heating also accelerated low molecular volatilization to form more foam pores and promoted cross-linking to stabilize foam growth [100]. Hence, microwave foaming has more obvious advantages than oven heating foaming as it can improve the toughness of MF by improving bubble structure.

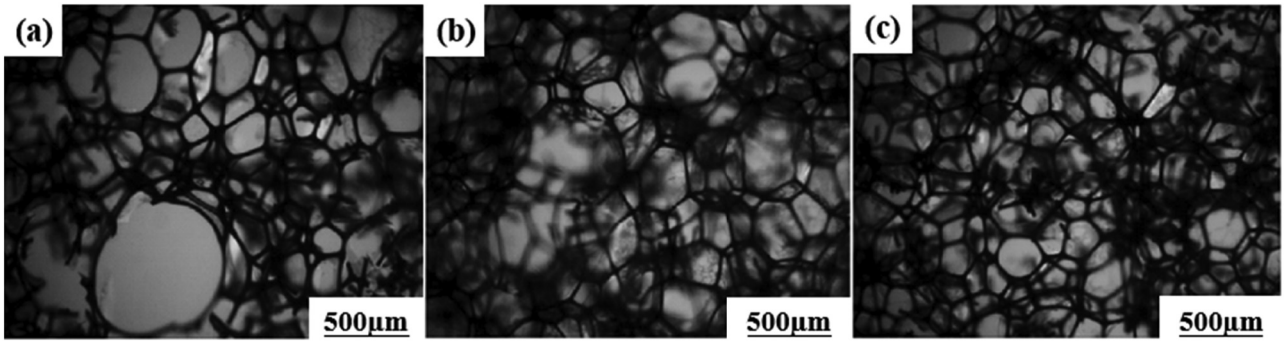

Figure 9: Micrograph of open-cell foams with different viscosities (η): (a) η = 40 mPa s, (b) η = 100 mPa s, and (c) η = 140 mPa s [100].

3.3 Foaming process

Microwave radiation power and radiation time have great influence on foam performance [104]. In the microwave foaming process, it is crucial for the MR to rapidly reach a high temperature within a short period of time. First, the foaming agent is rapidly vaporized under the action of high temperature and emulsifier to produce a large amount of foam, and solidified rapidly under the action of curing agent at the same time [105]. The MF with good comprehensive performance can be prepared only when the two processes of curing and foaming of resin are matched [43,106].

Wan *et al.* [105] investigated the effects of microwave power and foaming time on the structure and properties of MF foam. Figure 12 illustrates micrographs of MF at different microwave powers when an initial temperature of 25°C was maintained during a 60 s microwave foaming process. At a microwave power level of 1 kW h, the curing rate exceeded the foaming rate resulting in relatively thick skeleton structures within foam holes and higher foam density. Conversely, at a microwave power level of 3 kW h where the foaming rate surpassed the curing rate excessively, larger merged foam holes were observed with relatively fine skeleton structures within them as well as lower foam density. Only when using a microwave power level of 2 kW h did both foaming rate and curing rate match each other perfectly leading to highly uniform bubble holes in the foam.

Micrographs of the MF under different microwave times are presented in Figure 13, when the microwave power was set at 2 kW h. It can be observed from Figure 13 that excessive foaming time resulted in numerous cracks appearing in the foam structure. Conversely, if the foaming time was too short, incomplete curing and insufficient foam expansion occurred, potentially leading to severe shrinkage. The optimal foaming time was determined to be 60 s.

Therefore, in the process of MR foaming, the power and time of microwave radiation should be gradually regulated. In this way, the curing process and foaming process of resin can be matched, and MF with good comprehensive performance can be prepared.

3.4 Foaming agent and curing agent

Foaming agent and curing agent are two crucial additives in the foaming process of MR, which play a pivotal role in

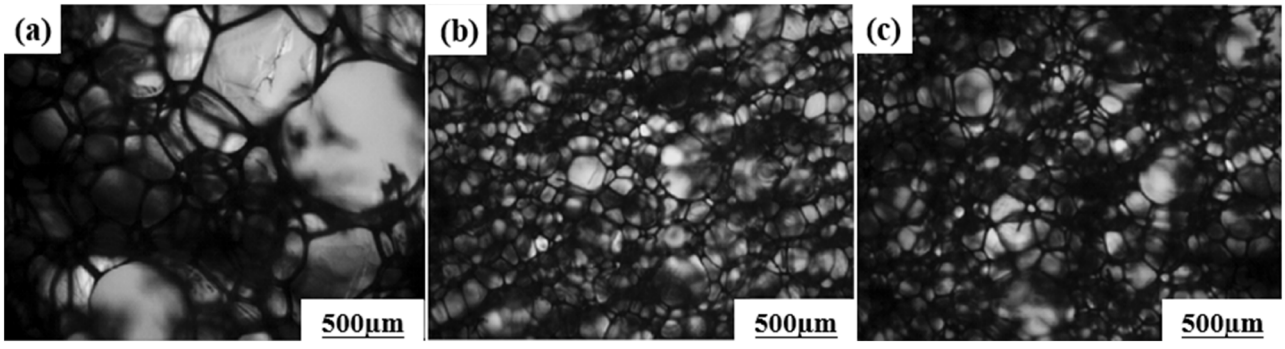

Figure 10: Micrograph of closed-cell foams with different viscosities (η): (a) η = 40 mPa s, (b) η = 100 mPa s, and (c) η = 140 mPa s [100].

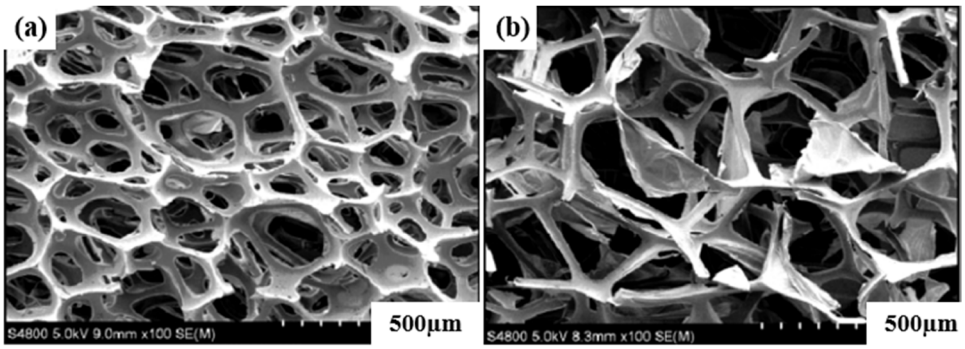

Figure 11: Morphology of MF produced by different foaming methods: (a) oven foaming and (b) microwave foaming [29,62].

maintaining foaming equilibrium [107,108]. The effect of foaming agent on the foam was mainly reflected on the foaming speed. Xia *et al.* [62] systematically investigated the effects of inorganic, organic, and compound foaming agents on the mechanical properties and flame retardancy of MF. The results showed that when $NaHCO_3$ was used as foaming agent, the performance of the foaming agent was better than that of other inorganic foaming agents. In terms of flammability: $NaHCO_3$ > Na_2CO_3 > organic foaming agent; in terms of mechanical properties, the mechanical properties of MF obtained by using chemical blowing agent diphenylmethane diisocyanate (MDI) were significantly better than other blowing agents, because MDI could be used not only as blowing agent but also as cross-linking curing agent, which greatly improved the mechanical properties of foam.

The curing agent's influence on the foam is mainly reflected in the curing speed. Generally speaking, when the curing rate surpasses the foaming rate, both the opening ratio and the length–diameter ratio will decrease and the bubble will collapse. Zhang *et al.* [108] reported the effect of the amount of formic acid (foaming agent) on the structures of the MF. It can be seen that excess formic acid decreased the opening rate (Figure 14a), and underuse increased the aspect ratio of the foam (Figure 14b).

Lei *et al.* [109] investigated the effects of the amount of foaming agent and curing agent on the apparent density and morphology of MF. The results demonstrated a direct influence of the foaming agent and curing agent quantities on the apparent density of MF (Figure 15). Excessive or insufficient amounts of foaming agent or curing agent led to an increase in foam's apparent density, as depicted in Figure 15. When there was an excess amount of foaming agent or a deficiency in curing agent, the foaming rate exceeded the curing rate, resulting in bubble fragmentation and consolidation, thereby increasing foam's apparent density. Conversely, when there was an excess amount of curing agent or a deficiency in foaming agent, the curing rate surpassed the foaming rate leading to inadequate foam expansion with more closed cells and increased apparent density. Optimal conditions for achieving light foam with uniform pore size and minimal apparent density were observed at 10% dosage for both foaming and curing agents relative to MR mass; this balanced ratio ensured similar rates between foaming and curing processes while enhancing MF toughness.

Hence, in the experimental design stage of MR foaming, the synergistic mechanism of foaming agent and curing agent should be carefully considered, so as to avoid the inconsistent phenomenon of foaming speed and curing speed, and then obtain MF with good toughness and low density.

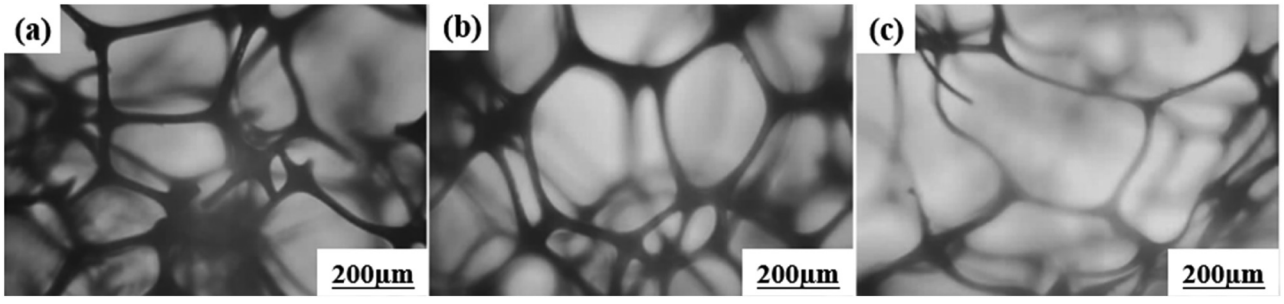

Figure 12: Micrographs of MF under different microwave powers; (a) 1 kW h, (b) 2 kW h, and (c) 3 kW h [105].

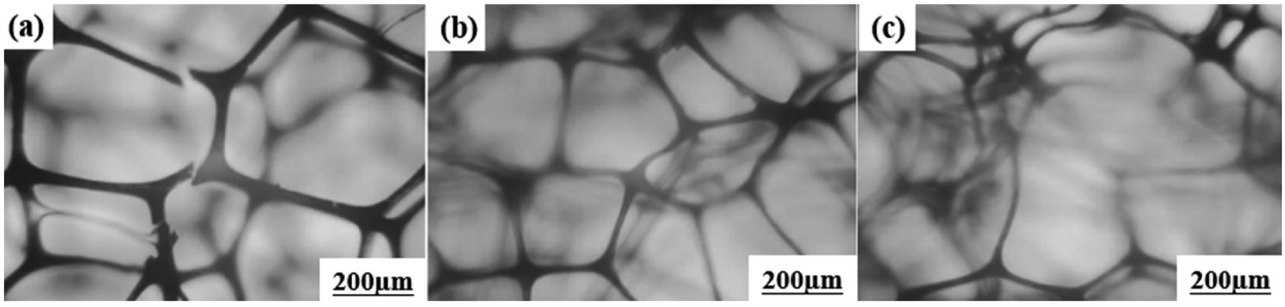

Figure 13: Micrographs of MF under different microwave time; (a) 30 s, (b) 60 s, and (c) 90 s [105].

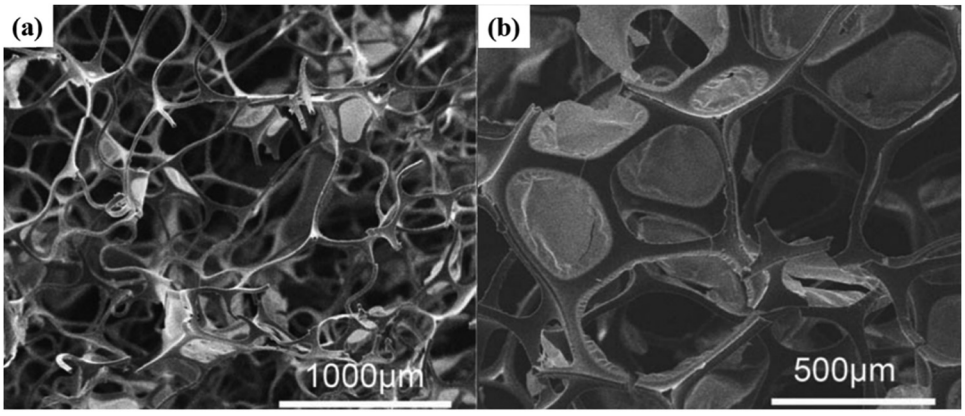

Figure 14: SEM micrographs of MFs. (a) The foam structure whose curing speed is slower than foaming speed and (b) the foam structure whose curing speed is faster than foaming speed [108].

3.5 Surfactant and other foaming AIDS

Surfactant is an important part of foam formation and stabilization until curing, and has a significant impact on the surface tension of the resin [104,106]. Too much surface tension of resin is not conducive to the formation of foam, and too little surface tension is not conducive to the stability of foam. Therefore, the amount of surfactant must be controlled in a certain range [100]. Thongkham *et al.* [110] proposed a flexible and lightweight thermoelectric material

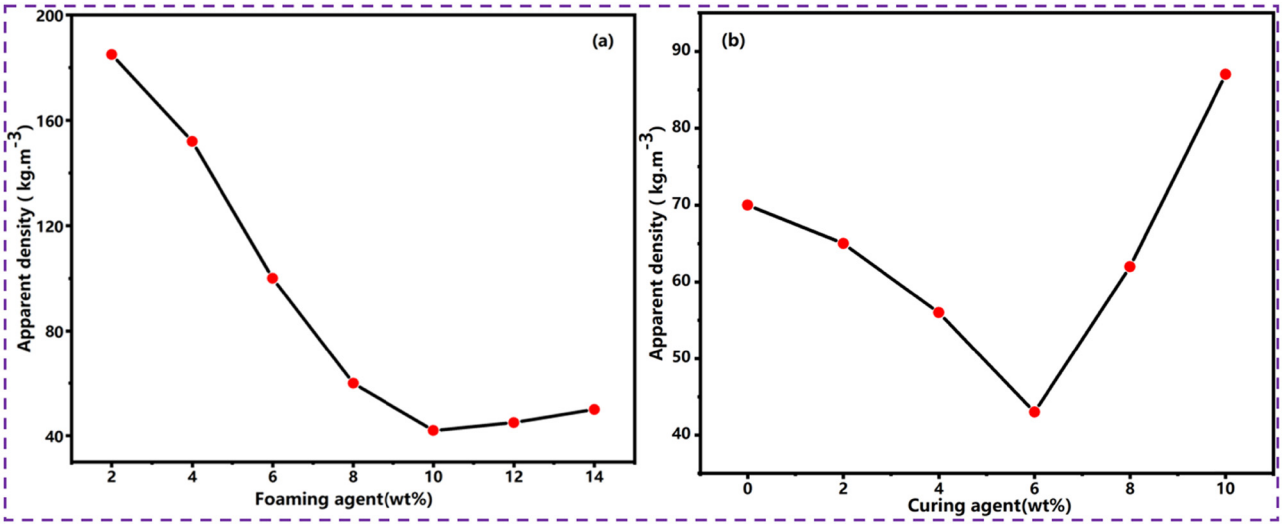

Figure 15: Effect of the mass fraction of foaming agent (a) and curing agent (b) on apparent density of MF [109].

developed on a MF using a simple dip-dry technique to self-assemble conductive nanofilms in the scaffold. Different amounts of poly(3,4-ethylenedioxythiophene):polystyrene-sulfonate conductive nanofilms were variedly fabricated in the foam due to altered amounts of sodium dodecyl sulfate (SDS) surfactant from 0 to 5 wt%. As a result, the highest nanofilm formation in the foam structure is achieved by adding 3 wt% SDS.

In addition to surfactant, some other additives also can be added to improve the foam performance during the foaming process of MR. Wang *et al.* [111] fabricated super-hydrophobic MF by *in situ* coprecipitation of hydrophobic SA@Fe_3O_4 (SA = stearic acid) nanoparticles on the surface of MF foam skeleton. Due to its low surface energy, high porosity, and large magnetic particles, the modified MF foam exhibits excellent super hydrophobicity, and oleophilic and magnetic responses.

Moreover, incorporating the MF into solvents during foaming completion represents an alternative approach to enhance the bubble structure and improve the toughness of MF. In order to improve the hydrophobic property of MF, Wang *et al.* [38] immersed the prepared MF in the aqueous solution of PVA. The results showed that PVA formed micro-nano structure on MF skeleton, which also improved the surface roughness and hydrophobic property. Compared with the complex methods and nanomaterials of traditional porous superhydrophobic adsorbents, the highly hydrophobic MF obtained by simple impregnation has better advantages in the treatment of oil spills and industrial organic pollution.

3.6 Comprehensive regulation analysis of MF pore structure

In summary, the effect of the bubble structure of MF properties is as important as that of the molecular structure of MR. In order to obtain the MF with uniform foam holes, small density, and good mechanical properties, the physical properties (viscosity and solid content), foaming method (oven foaming and microwave foaming), foaming time, and power of the resin solution are the key effect factors in the foaming process. In addition, the foaming speed (foaming agent), curing speed (curing agent), and surfactants are also the important effect elements of MF processing. By adjusting the content of foaming agent, curing agent, and surfactant, the MF pore structure and density can be well regulated and controlled. It is worth noting that the microwave foaming has more obvious advantages than oven heating foaming, which can improve the toughness of MF by improving the bubble structure and should be further studied. The influencing factors of MF pore structure and MR molecular structure are shown in Figure 16.

4 Extended application of MF foam

As previously mentioned, MF has the features of excellent flame retardance, good sound absorption property, low density, and high opening, these characteristics enable

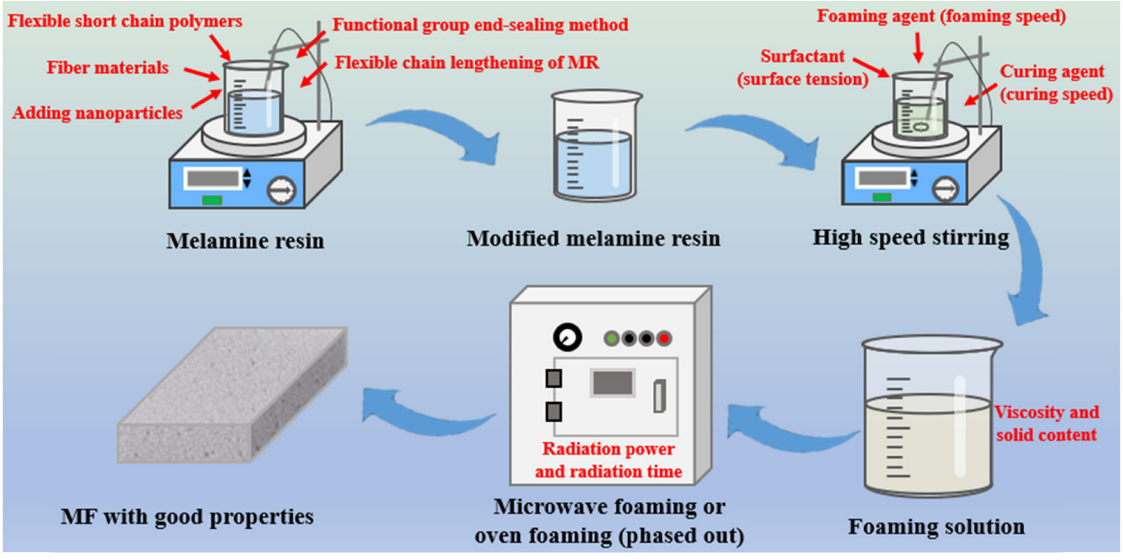

Figure 16: The influencing elements of MR molecular structure and MF pore structure.

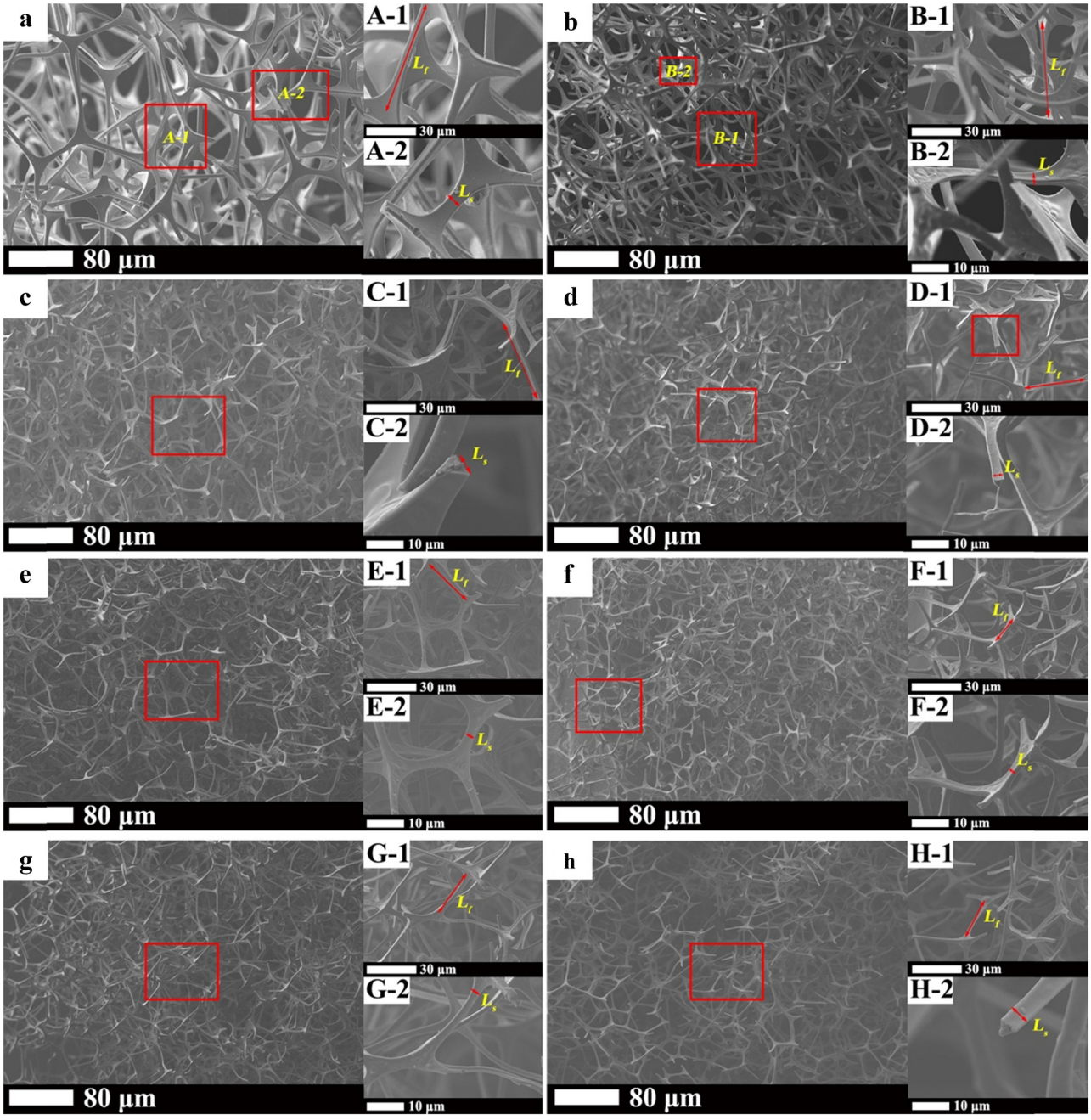

Figure 17: Microstructures of carbon foam samples were obtained at different pyrolysis temperatures. (a) MF, (b) 450°C, (c) 550°C, (d) 650°C, (e) 750°C, (f) 850°C (g) 950°C, and (h) 1,050°C.

MF to be successfully applied in the fields of oil and water separation, VIP, building materials, and automotive sound-proofing materials. With the continuous exploration of experts and scholars, the application scope of MF has been gradually expanded. This chapter will summarize the two main extended application areas (carbon foam and carbon aerogel [112,113]) of MF foam.

4.1 Carbon foam

4.1.1 Thermal insulation

Carbon foams, which can be produced through direct carbonization of MF, exhibit promising potential in supporting thermal insulation systems due to their exceptional

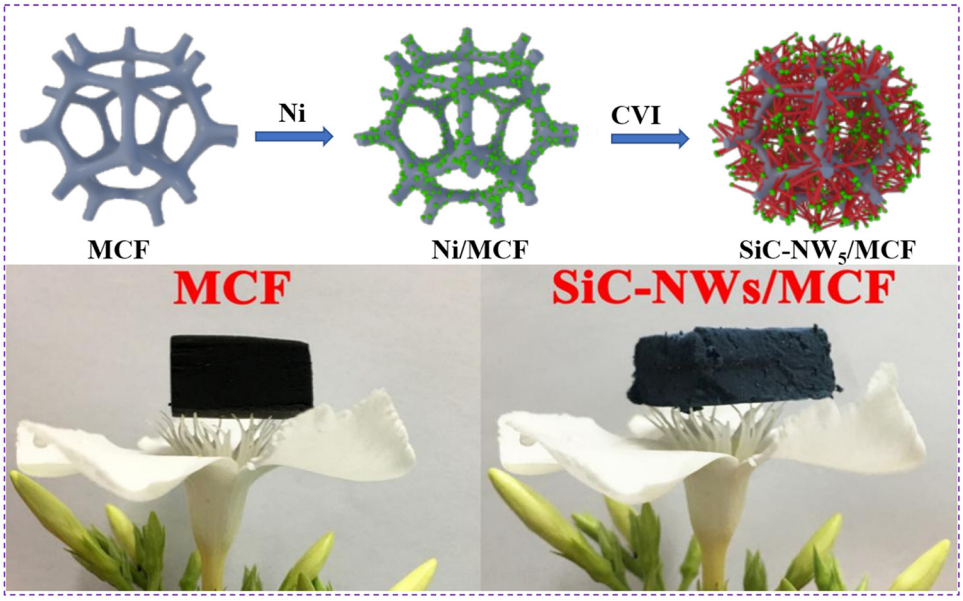

Figure 18: Preparation of SiC nanowires-reinforced MCF foams [119].

form-stable characteristics in photothermal conversion and storage [114–116]. For instance, the pyrolysis process of carbon foam matrices prepared from MFs was investigated by Chen's team at Nanjing University of Aeronautics and Astronautics [117,118]. The SEM images presented in Figure 17 depict the microstructure of carbon foam under various pyrolysis temperatures ranging from 450 to 1,050°C. As can be seen from Figure 17a, the pore size of the non-pyrolyzed dense amine foam sample was large, with the pore size ranging from 100 to 200 μm, and the pore wall was thick and long. However, with the increase in the pyrolysis temperature, the pore structure participation of the prepared carbon foam was obviously different from that of the dense amine foam sample. As shown in Figure 17b–f, it can be clearly seen that the carbon foam still maintained the three-dimensional mesh open-pore skeleton structure in the MF sample. However, with the increase in the pyrolysis temperature, the number of three-dimensional mesh pores in the field of view enhanced significantly, and the corresponding pore size also shrank gradually, from 100–200 to 20–80 μm in the sample of dense amine foam. At the same time, the pore wall of carbon foam gradually became more thinner and shorter. The small pores in the three-dimensional network increased the scattering, reflection, and absorption of radiation energy passing through the porous structure, and effectively reduced the thermal conductivity of melamine-derived carbon foam (MDCF) samples.

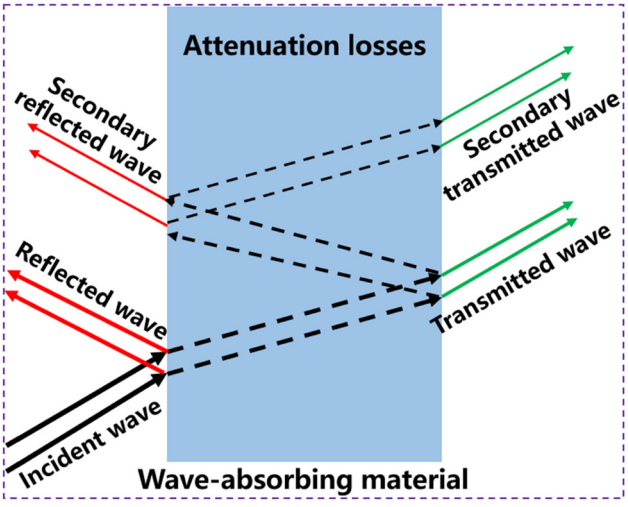

Figure 19: Electromagnetic wave and material interaction principle.

In the previous work of Chen *et al.* [117,118], the influence of SiC nanowire parameters on the structure and properties of composite foam under various chemical vapor infiltration processes (Figure 18) was investigated. A novel type of Sic nanowire-reinforced carbon foam composites was proposed, which was composed of a carbon foam matrix as well as the filled SiC nanowires in the carbon foam, with an average pore diameter of 12–14 nm and a thermal conductivity of 0.036 W/(m K) at 100°C and 0.243 W/(m K) at 900°C. And, its bulk density can be as low as 5.56 mg/cm^3. At present, the stabilization carbon foam has been successfully applied in the first-generation rover insulation board as reinforcing material. And it also has passed all of the technical indicators assessment requirements of the China academy of space technology, Beijing satellite manufacturer Co., Ltd.

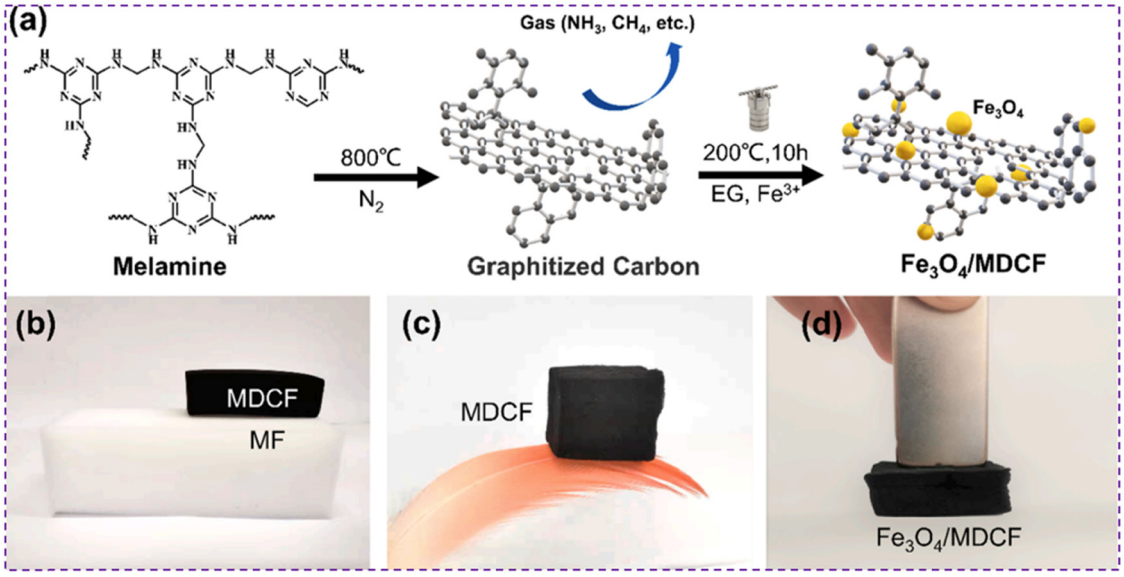

Figure 20: (a) Carbonization and synthetic process of Fe_3O_4/MDCF composite, (b) optical photograph of MF and MDCF, (c) an ultralight MDCF standing on feather, and (d) Fe_3O_4/MDCF composite is attracted by a magnet [123].

The SiC nanowire-reinforced carbon foams have provided help for implementation of the Mars exploration program and the successful launch of the "Tianwen" Mars exploration rover.

4.1.2 Electromagnetic wave absorption materials

Carbon foam made of MF is not only used in thermal insulation systems of spacecraft, but also widely used in electromagnetic wave absorption materials due to its high porosity and low density [24,120,121]. Lyu *et al.* [122] constructed a three-dimensional carbon foam material embedded with CuNi alloy nanoparticles for electromagnetic wave absorption. In the synthetic procedure, Ni^{2+} and Cu^{2+} were first adsorbed into the MF to form Ni^{2+}–Cu^{2+}/MF composites, which were then subject to the pyrolysis treatment, resulting in the production of mesoporous CuNi alloy/CF. The experiment results showed that the CuNi/CF with CuNi alloy nanoparticles evenly distributed in the 3D carbon matrix inherits the characteristic of the 3D structured N-rich MF, which induces masses of dipole polarization, interfacial polarization, and electromagnetic wave scattering. The $CuNi_{11}$ exhibited excellent electromagnetic wave absorption and insulation performance with the reflection loss (RL) of −50.20 dB at a thin thickness of 1.6 mm. The electromagnetic wave and wave-absorbing material interaction principle is shown in Figure 19.

Jiang *et al.* [123] synthesized the ferroferric oxide/MDCF (marked as Fe_3O_4/MDCF) by carbonization and *in situ* growth strategy. The results showed that the minimum values of RL, the effective frequency width of absorption, and the density of the Fe_3O_4/MDCF were −26.45 dB (7.76 GHz), 4.28 GHz, and 13.1 mg/cm^3, respectively. The continuous 3D (three dimensional) conductive network and the expanded

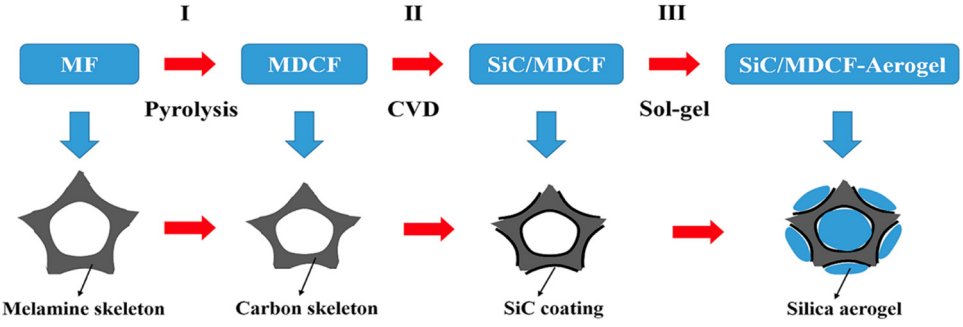

Figure 21: Manufacturing processes of SiC/MDCF–Aerogel. The main conclusions were as follows:.

Table 5: Single performance index corresponding to the optimal comprehensive performance

Number	Rate of change of volume density (%)	Compression modulus (kPa)	Absorbing ability (kJ/m^3)	Specific energy absorption (kJ/kg)
Optimal performance	28.81	204.14	7.05	1.63

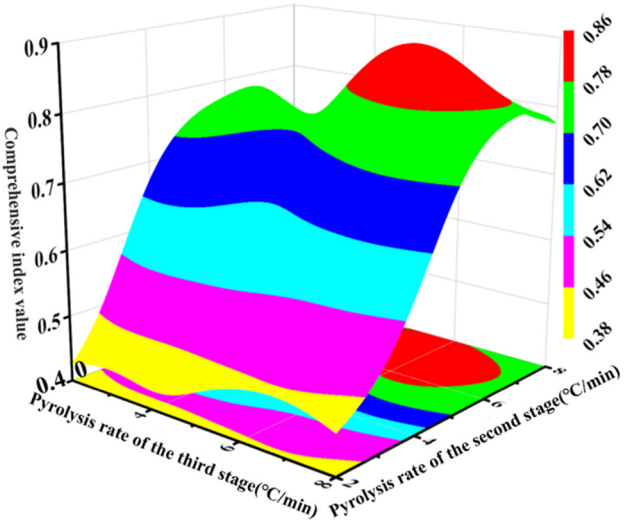

Figure 22: The three-dimensional surface diagram of comprehensive performance index of carbon foam.

interface in the carbon/magnetic heterostructure improved the interfacial polarization relaxation, and enhanced the electromagnetic loss and wave absorbing capability. The preparation process of the Fe_3O_4/MDCF, the physical photos of the MF, and the Fe_3O_4/MDCF composite are shown in Figure 20.

4.2 Aerogel areas

Carbon aerogel is a prominent area of MF expansion in the field of multifunctional material [124–128]. With the growing complex operating environment of the modern weapon systems, the electromagnetic interference phenomenon has become an increasingly serious concern as a single performance index cannot meet the usage requirements of the highly sophisticated field for performance optimization and functional pluralism materials. In line with this perspective, Chen *et al.* [129–139] proposed a carbon/silicon carbide/silica aerogel composite with lightweight, high strength, heat insulation, and microwave absorption performances. The carbon foam matrix made of MF was optimized using a segmented pyrolysis process and a neural network model. Then, the uniform silicon carbide coating was deposited on the surface of the carbon foam skeleton by the chemical vapor deposition technology to prepare the carbon/silicon carbide foam. Finally, the silica aerogel was filled in the pores of the carbon/silicon carbide foam by the sol–gel technique, resulting in the carbon/silicon carbide/silica aerogel composite after drying under normal pressure. The manufacturing process is shown in Figure 21.

1) The structure and performance of melamine-based carbon foam was primarily determined by the pyrolysis process, and the constructed backpropagation neural network model can optimize the pyrolysis process of carbon foam to obtain the carbon foam with the best comprehensive performance. The single performance index corresponding to the optimal comprehensive performance is shown in Table 5, and the three-dimensional surface diagram of comprehensive performance index of carbon foam is depicted in Figure 22.

2) The silicon carbide coating on the surface of carbon foam can be prepared *via* a chemical vapor deposition

Table 6: Electromagnetic absorbing performance of silicon carbide matrix composites

Samples	Min RL (dB)	Min frequency (GHz)	Min matching thickness (mm)	Effective absorption band (GHz)	Reference
C/SiC-16h	−29.74	11.12	1.75	3.62	[132,133]
C/SiC-T900	−51.58	8.96	3.60	10.84	[131,132]
SiC_{fiber}/SiC	−47.50	11.40	2.50	2.80	[140]
SiC aerogel	−43.00	13.00	2.00	4.00	[141]
SiC nanowire foam	−49.10	12.20	2.85	4.20	[142]
Graphite/SiC aerogel	−47.30	10.52	3.00	4.70	[143]
SiC mixed carbon foam	−43.20	4.70	5.00	4.00	[144]

Table 7: Comparison of absorbing properties of SiC/SiO_2 composites

Samples	Min RL (dB)	Min frequency (GHz)	Min matching thickness (mm)	Effective absorption band (GHz)	Reference
$C/SiC/SiO_2$-T900	−55.38	16.56	2.85	8.16	[129]
Fe-SiC/SiO_2	−32.00	9.00	3.25	4.20	[145]
SiC/SiO_2 composites	−52.00	10.80	~3.00	4.20	[146]
SiC/SiO_2-1400	−52.00	10.80	2.75	4.00	—
SiC/SiO_2 core-shell nanowires	−32.72	13.84	3.00	5.32	[147]
Activated carbon-based C/SiC/SiO	−30.80	~15.20	1.50	~4.80	—

process. The thickness of silicon carbide coating significantly influences the structure and mechanical properties, dielectric properties, and wave absorption properties of carbon/silicon carbide foam, and the heat treatment temperature can improve the properties of carbon/silicon carbide foam. The electromagnetic absorbing performances of silicon carbide matrix composites are shown in Table 6. Compared with the current traditional silicon carbide fiber or silicon carbide matrix, the C/SiC-T900 foam after 900°C heat treatment had lower minimum RL and wider effective absorption band, so it showed better microwave absorption performance, and had great application potential in the future military or civil microwave absorption system.

3) The sol–gel process employed for the preparation and infiltration of aerogel into the pores of carbon/silicon carbide foam. The structure and properties of carbon/silicon carbide/silicon dioxide aerogel are affected by the thickness of silicon carbide coating, and the heat treatment temperature can improve the properties of carbon/silicon carbide/silicon dioxide aerogel. The comparison of absorbing properties of SiC/SiO_2 composites are shown in Table 7. It can be found that the $C/SiC/SiO_2$-T900 aerogel obtained by heat treatment at 900°C had lower minimum RL, wider effective absorption band, better microwave absorption performance, and great application potential.

In addition to this study, many other scholars have also reported the applications of carbon aerogel made with MF. Such as Wang *et al.* [113] reported a very facile approach for the preparation of compressible, fatigue resistant, conductive, and pressure-sensitive carbon aerogels by pyrolysis of cellulose nano-fibers aerogel using MF as the skeleton. The resulting carbon aerogels exhibit excellent performance, including a low density of 11.23 mg/cm^3, high electrical conductivity of 0.378 S/cm, high sensitivity, and outstanding mechanical properties. Moreover, the high nitrogen content and hydrophilic property enable the carbon aerogels to be used as compressible electrodes with a specific and areal capacitance of 92.2 F/g and 461 mF/cm^2, respectively, showing the promising prospect of flexible supercapacitors. The specific applications of carbon aerogel prepared by MF are shown in Table 8.

Table 8: Specific application of carbon aerogel prepared by MF

Applications	Methods or process	Properties
MXene-based aerogel areas [125]	Using MF as a robust template for MXene/reduced graphene oxide aerogel	High solvent absorption capacity, great electrothermal conversion rate, and good photothermal conversion ability
Solar energy utilization areas [127]	Sol–gel polymerization, freeze drying, and carbonization	Excellent thermal stability and high thermal storage density
Organic absorption and high-temperature thermal insulation areas [128]	Sol–gel polymerization, ambient pressure drying, and co-carbonization	High compressive strength, ultra-low thermal conductivity, and high-volume organic absorption capability
Electromagnetic wave absorption materials [129]	Pyrolysis, sol–gel method, and chemical vapor deposition	Excellent microwave absorption performance
Flexible supercapacitors [113]	Using MFs as the skeleton, and pyrolysis cellulose nanofibers aerogel	Low density, outstanding mechanical properties, high electrical conductivity, and sensitivity
Supercapacitor (nitrogen-doped carbon aerogel) [148]	Direct pyrolysis of bamboo cellulose nanofibers/melamine/graphene oxide hybrid aerogel	Superior mechanical durability and excellent electrochemical stability

5 Conclusion

Due to its excellent sound absorption, heat resistance, and preservation properties, as well as low density, MF has been widely utilized in the preparation of oil–water separation materials, supercapacitors, sound absorption materials, and vacuum insulated panels in recent years. However, its own shortcomings of MF such as hardness, poor toughness, fragility, and slag removal greatly limit its application scope. Therefore, this review addressed the recent toughening modification methods and application areas of MF. Specifically, future research should explore the following four aspects of MF toughening modification.

1) Exploring cost-effective modifiers and determining the optimal dosage to reduce the crosslink density of MR, thereby enhancing the toughness of MF without compromising its flame retardant and heat resistance properties.
2) By integrating different toughening and modification methods in accordance with specific application requirements, incorporating flexible chain segments with excellent properties into MR can lead to the synthesis of composite modified MF with improved toughness.
3) Optimizing the synthesis process and foaming process of MR from the perspectives of simplifying production procedures and reducing costs, aiming to enhance foam quality by achieving low density and uniform bubble pores.
4) Continuously advancing research on MF modification mechanisms to facilitate functionalization and refinement, thus promoting further development in this field.

Moreover, considering the low density, high porosity, and exceptional heat insulation characteristics of MF, it is imperative to further investigate the potential application of carbon foam and aerogel derived from MF in the aviation industry and electromagnetic wave absorption field. It is anticipated that through extensive research on MF synthesis, foaming technology advancements, and nanotechnology developments, there will be continuous enhancements in the mechanical properties, microwave absorbing capabilities, and thermal insulation performance of MF derivatives. Consequently, commercialization and serialization of MDCF and aerogel can be expected in the near future.

Funding information: This research work was supported by National Natural Science Foundation of China (U2167214, 92160202, and 51905268), the National Key Research and Development Program of China (2021YFB3703100), Science and Technology International Cooperation Project of Jiangsu (BZ2021055), Industry Foresight and Key Core Technology Competition Project of Jiangsu (BE2022147), and the Overseas Professor Project (G2022181024L).

Author contributions: Methodology, conceptualization, and project administration: Z.C. and L.Y.; writing original draft and visualization: Y.W. and Y.L; writing – review and editing: Y.W. and Z.C.; funding acquisition and resources: T.X., H.W., L.H., and J.Z.; supervision: Z.C. and L.Y. All authors have accepted responsibility for the entire content of this manuscript and approved its submission.

Conflict of interest: The authors declare that they have no known competing financial interests or personal relationships that could have appeared to influence the work reported in this article.

References

[1] Hailan SM, Ponnamma D, Krupa I. The separation of oil/water mixtures by modified melamine and polyurethane foams: A review. Polymers. 2021;13(23):4142.
[2] Yang J-C, Cao Z-J, Wang Y-Z, Schiraldi DA. Ammonium polyphosphate-based nanocoating for melamine foam towards high flame retardancy and anti-shrinkage in fire. Polymer. 2015;66:86–93.
[3] Guo T, Chen XL, Su L, Li CG, Huang XZ, Tang XZ. Stretched graphene nanosheets formed the “obstacle walls” in melamine sponge towards effective electromagnetic interference shielding applications. Mater Des. 2019;182:108029.
[4] VanDercreek C, Avallone F, Ragni D, Snellen M. Simulating the acoustic response of cavities to improve microphone array measurements in closed test section wind tunnels. J Acoust Soc Am. 2022;151:322–33.
[5] Duan HN, Lyu HH, Shen BX, Tian JY, Pu XY, Wang FM, et al. Superhydrophobic-superoleophilic biochar-based foam for high-efficiency and repeatable oil–water separation. Sci Total Environ. 2021;780:146517.
[6] Zhou X, Liu Y, Wang Y, Gao P, Liu W. Influence of various factors on vertical combustibility of polyurethane rigid foam. China Plast. 2012;26:77–81.
[7] Xiao F, Zhang HX, Wu TZ, Liu JH, Liu JX, Zhang JB, et al. Superhydrophobic/superlipophilic interface layer for oil–water separation. Process Saf Environ Prot. 2022;161:13–21.
[8] Ma JJ, Xie YC, Yang T, He XH. Melamine foam with pH-responsive wettability for fast oil absorption and desorption. Adv Mater Interfaces. 2022;9(10):2102092.
[9] Zhao M, Nie JH, Li H, Xia MY, Liu MY, Zhang ZL, et al. High-frequency supercapacitors based on carbonized melamine foam as energy storage devices for triboelectric nanogenerators. Nano Energy. 2019;55:447–53.
[10] Zhao YL, Wang AJ, Shen LZ, Zhao ZK, Xiao LQ, Hou LX. Nitrogen, sulfur co-doped porous carbon via high internal phase emulsion template and its potential application as the electrode of high-performance supercapacitor. J Appl Polym Sci. 2022;139(25):e52417.

[11] Shen L, Zhang HR, Lei YZ, Chen Y, Liang M, Zou HW. Hierarchical pore structure based on cellulose nanofiber/melamine composite foam with enhanced sound absorption performance. Carbohydr Polym. 2021;255:117405.
[12] Yan C, Luo YJ, Zhang WG, Zhu ZF, Li PY, Li N, et al. Preparation of a novel melamine foam structure and properties. J Appl Polym Sci. 2022;139(16):51992.
[13] Nemanic V, Zajec B, Zumer M, Figar N, Kavsek M, Mihelic I. Synthesis and characterization of melamine-formaldehyde rigid foams for vacuum thermal insulation. Appl Energy. 2014;114:320–6.
[14] Duan C, Zou W, Du Z, Li H, Zhang C. Fabrication of micro-mesopores in macroporous poly (formaldehyde-melamine) monoliths via reaction-induced phase separation in high internal phase emulsion template. Polymer. 2019;167:78–84.
[15] Dorieh A, Pour MF, Movahed SG, Pizzi A, Selakjani PP, Kiamahalleh MV, et al. A review of recent progress in melamine-formaldehyde resin based nanocomposites as coating materials. Prog Org Coat. 2022;165:106768.
[16] Sakhadeo NN, Patro TU. Exploring the multifunctional applications of surface-coated polymeric foams-A review. Ind Eng Chem Res. 2022;61:5366–87.
[17] Sun HD, Liu ZM, Liu KY, Gibril ME, Kong FG, Wang SJ. Lignin-based superhydrophobic melamine resin sponges and their application in oil/water separation. Ind Crop Prod. 2021;170:113798.
[18] Samanta P, Samanta A, Montanari C, Li YY, Maddalena L, Carosio F, et al. Fire-retardant and transparent wood biocomposite based on commercial thermoset. Compos Part A-Appl Sci Manuf. 2022;156:106863.
[19] Arumugam H, Ismail AAM, Govindraj L, Muthukaruppan A. Development of bio-based benzoxazines coated melamine foam for oil–water separation. Prog Org Coat. 2021;153:106128.
[20] Li M, Fang YF, Liu C, Zhou MM, Miao XM, Pei YB, et al. Facile generation of highly durable thiol-functionalized polyhedral oligomeric silsesquioxane based superhydrophobic melamine foam. Front Chem Sci Eng. 2022;16:1247–58.
[21] Hentati C, Job S, Crete JP, Taktak M, Haddar M, Dauchez N. On the contact law of open-cell poro-granular materials. Int J Solids Struct. 2021;208:83–92.
[22] Wu LF, Wang L, Sun SH, Sun XN. Hybrid active and passive noise control in ventilation duct with internally placed microphones module. Appl Acoust. 2022;188:108525.
[23] Wu XW, Lei YG, Li SH, Huang JY, Teng L, Chen Z, et al. Photothermal and Joule heating-assisted thermal management sponge for efficient cleanup of highly viscous crude oil. J Hazard Mater. 2021;403:124090.
[24] Xiao YY, He YJ, Wang RQ, Lei YZ, Yang JH, Qi XD, et al. Mussel-inspired strategy to construct 3D silver nanoparticle network in flexible phase change composites with excellent thermal energy management and electromagnetic interference shielding capabilities. Compos Part B-Eng. 2022;239:109962.
[25] Wei YC, Wang MF, Qi W, He ZM. Flame-resistant bifunctional MOF-based sponges for effective separation of oil/water mixtures and enzyme-like degradation of organic pollutants. Process Saf Environ Prot. 2022;163:636–44.
[26] Huang T, Cao S, Luo D, Zhang N, Lei YZ, Wang Y. Polydopamine-assisted polyethylenimine grafting melamine foam and the application in wastewater purification. Chemosphere. 2022;287:132054.
[27] Du MY, Guo CL, Cai YB, Liu JY, Wei QF, Li LG. Multifunctional shape-stabilized phase change composites based upon multi-walled carbon nanotubes and polypyrrole decorated melamine foam for light/electric-to-thermal energy conversion and storage. J Energy Storage. 2021;43:103187.
[28] Naikwadi AT, Samui AB, Mahanwar PA. Fabrication and experimental investigation of microencapsulated eutectic phase change material-integrated polyurethane sandwich tin panel composite for thermal energy storage in buildings. Int J Energy Res. 2021;45:20783–94.
[29] Wang D, Zhang X, Luo S, Zhao Q, Li S. Study of preparation and modification and properties of melamine formaldehyde resin foam. J Funct Mater. 2012;43:3381–5.
[30] VanDercreek C, Merino-Martinez R, Sijtsma P, Snellen M. Evaluation of the effect of microphone cavity geometries on acoustic imaging in wind tunnels. Appl Acoust. 2021;181:108154.
[31] Yang Y, Chen Z, Xu TZ, Han RN, Awuye DE. Sound insulation and hydrophobic properties of phenolic resin modified melamine foam: role of micro-morphology. Mater Res Express. 2019;6:075331.
[32] Li DK, Jiang ZC, Li L, Liu XB, Wang XF, He M. Investigation of acoustic properties on wideband sound-absorber composed of hollow perforated spherical structure with extended tubes and porous materials. Appl Sci.-Basel. 2020;10(24):8978.
[33] Li B, Ding HY, Hu ZG, Zhao JY, Qi MH, Wang ZY. Simulation analysis of the sound transmission loss of composite laminated cylindrical shells with applied acoustic coverings. Shock Vib. 2022;2022:1084738.
[34] Nine MJ, Ayub M, Zander AC, Tran DNH, Cazzolato BS, Losic D. Graphene oxide-based lamella network for enhanced sound absorption. Adv Funct Mater. 2017;27(46):1703820.
[35] Liu L, Chen YJ, Liu HZ, Rehman HU, Chen C, Kang HM, et al. A graphene oxide and functionalized carbon nanotube based semi-open cellular network for sound absorption. Soft Matter. 2019;15:2269–76.
[36] Pinto J, Athanassiou A, Fragouli D. Surface modification of polymeric foams for oil spills remediation. J Environ Manag. 2018;206:872–89.
[37] Mu L, Yue X, Hao B, Wang R, Ma PC. Facile preparation of melamine foam with superhydrophobic performance and its system integration with prototype equipment for the clean-up of oil spills on water surface. Sci Total Environ. 2022;833:155184.
[38] Wang XT, Han ZQ, Liu Y, Wang Q. Micro-nano surface structure construction and hydrophobic modification to prepare efficient oil–water separation melamine formaldehyde foam. Appl Surf Sci. 2020;505:144577.
[39] Li M, Bian C, Yang GX, Qiang XH. Facile fabrication of water-based and non-fluorinated superhydrophobic sponge for efficient separation of immiscible oil/water mixture and water-in-oil emulsion. Chem Eng J. 2019;368:350–8.
[40] Xue F, Lu Y, Qi XD, Yang JH, Wang Y. Melamine foam-templated graphene nanoplatelet framework toward phase change materials with multiple energy conversion abilities. Chem Eng J. 2019;365:20–9.
[41] Li CW, Jiang DG, Huo BB, Ding MC, Huang CC, Jia DD, et al. Scalable and robust bilayer polymer foams for highly efficient and stable solar desalination. Nano Energy. 2019;60:841–9.
[42] Qiu XQ, Wang DQ, Li Q, Li XY, Zhao XW, Li ZW, et al. Reutilization of melamine-formaldehyde foam wastes: Removing Sn^{2+} in simulated

tin-containing wastewater to transform a fire hazard suppressant of flexible poly(vinyl chloride). J Appl Polym Sci. 2022;139(9):51724.
[43] Wang X, Ma H, Song C, Zhou Z, Xu W, Ren F, et al. Preparation and performance of high-strength flame retardant rigid melamine foam materials. Polym Mater Sci Eng. 2019;35:153–9.
[44] Bondar KE, Laponov SV, Suleymanov DF, Shulaev NS. Models of temperature fields and their influence on polymeric coating adhesion. Iop; 2020.
[45] Grabmann MK, Wallner GM, Grabmayer K, Nitsche D, Lang RW. Aging behavior and lifetime assessment of polyolefin liner materials for seasonal heat storage using micro-specimen. Sol Energy. 2018;170:988–90.
[46] Momanyi J, Herzog M, Muchiri P. Analysis of thermomechanical properties of selected class of recycled thermoplastic materials based on their applications. Recycling (Switz). 2019;4:33 (16 pp.).
[47] Shi Y, Zhou B. Melamine foam impregnated with paraffin as thermal regulation materials for obtaining stable indoor temperature. Energy Build. 2019;183:650–8.
[48] Mareze PH, Brandao E, Fonseca WD, Silva OM, Lenzi A. Modeling of acoustic porous material absorber using rigid multiple microducts network: Validation of the proposed mode. J Sound Vib. 2019;443:376–96.
[49] Li CH, Ma HH, Song CQ, Zhou ZF, Xu WB, Song QS, et al. Preparation and performance of melamine-formaldehyde rigid foams with high closed cell content. Cell Polym. 2021;40:183–97.
[50] Kavsek M, Figar N, Mihelic I, Krajnc M. Melamine-formaldehyde rigid foams - Manufacturing and their thermal insulation properties. J Cell Plast. 2022;58:175–93.
[51] Liu JX, Zhou L, Jiang QB, Yang J, Xie JJ. Synthesis and characterization of melamine-formaldehyde resin for foaming use. 2014;24–7.
[52] Kan YF, Sun B, Kan HF, Bai YM, Gao ZH. Preparation and characterization of a melamine-urea-glyoxal resin and its modified soybean adhesive. Int J Adhes Adhes. 2021;111:102986.
[53] Liu XJ, Guo YW, Zheng JF, Wu J, Hu B. Preparation of hexamethylol melamine resin with low crystallization water and low viscosity for hexamethylol melamine/polyvinyl alcohol composite membrane. Pol J Chem Technol. 2022;24:47–56.
[54] Shokri A. Using Mn based on lightweight expanded clay aggregate (LECA) as an original catalyst for the removal of NO_2 pollutant in aqueous environment. Surf Interfaces. 2020;21:100705.
[55] Liu M, Zhang C, Du ZJ, Zou W. Fabrication of shape-stabilized phase change materials with melamine foam/multi-walled carbon nanotubes composite as container. Compos Interfaces. 2021;28:255–71.
[56] Zhang H, Zhou Y, Li CG, Chen SL, Liu L, Liu SW, et al. Porous nitrogen doped carbon foam with excellent resilience for self-supported oxygen reduction catalyst. Carbon. 2015;95:388–95.
[57] Wascher R, Avramidis G, Viol W. Plywood made from plasma-treated veneers: Investigation of performance differences between plasma-pretreated and untreated beech veneers at comparable melamine resin load. Forests. 2021;12.
[58] Xu W, Wu X, Shi B. Toughening agent for melamine formaldehyde resin: A new method for recycling chrome shavings. Polymer. 2022;253:124979.
[59] Jeong B, Park BD, Causin V. Influence of synthesis method and melamine content of urea-melamine-formaldehyde resins to their features in cohesion, interphase, and adhesion. J Ind Eng Chem. 2019;79:87–96.
[60] Zhang XY, Gu Z, Sui JY, Li ZX, Song LN, Yang LN, et al. Preparation and characterization of halogen-free flame retardant MCA core-shell microcapsules coated with melamine or acrylic acid resin. Polimery. 2021;66:245–52.
[61] Li CF, Qin ZX, Liu Y, Pan YD, Liu ML. Preparation of a nano-silica modified melamine formaldehyde resin. Int J Adhes Adhes. 2022;113:103076.
[62] Xia X, Gu X, Feng L, Wang J, Zhang C. Advances on Toughening Modification of Melamine Foam. Polym Mater Sci Eng. 2019;35:182–90.
[63] Bal A, Acar I, Guclu G. A novel type nanocomposite coating based on alkyd-melamine formaldehyde resin containing modified silica: Preparation and film properties. J Appl Polym Sci. 2012;125:E85–92.
[64] Li CH, Ma HH, Zhou ZF, Xu WB, Ren FM, Yang XY. Preparation and properties of melamine-formaldehyde rigid closed-cell foam toughened by ethylene glycol/carbon fiber. Cell Polym. 2021;40:55–72.
[65] Han RL, Zhang YF. Studies on performance of cured water-borne melamine-acrylic emulsion coatings. J Adhes Sci Technol. 2011;25:883–92.
[66] Hang ZS, Tan LH, Cao XM, Ju FY, Ying SJ, Xu FM. Preparation of melamine microfibers by reaction electrospinning. Mater Lett. 2011;65:1079–81.
[67] Su C, Wang X, Wu ZS. Enhancement of mechanical properties of FRP composites with silica nanoparticles; 2021. p. 684–94.
[68] Sun YF, Wang YP, Mu WL, Zheng ZP, Yang B, Wang JW, et al. Mechanical properties of 3D printed micro-nano rice husk/polylactic acid filaments. J Appl Polym Sci. 2022;139(28):e52619.
[69] Pan S, Upadhyay R, Singh S, Singh M. Synthesis, characterization, and functionalization of superadhesive melamine formaldehyde polyvinylpyrrolidone resins doped with metallic and graphene oxide nanoparticles for better industrial applications. J Appl Polym Sci. 2022;139(38).
[70] Binyaseen AM, Bayazeed A, Al-nami SY, Abu Al-Ola K, Alqarni SA, Abdel-Hafez SH, et al. Development of epoxy/rice straw-based cellulose nanowhiskers composite smart coating immobilized with rare-earth doped aluminate: Photoluminescence and anticorrosion properties for sustainability. Ceram Int. 2022;48:4841–50.
[71] Javed R, Zia M, Naz S, Aisida SO, Ul Ain N, Ao Q. Role of capping agents in the application of nanoparticles in biomedicine and environmental remediation: recent trends and future prospects. J Nanobiotechnol. 2020;18.
[72] Miao SJ, Xu J, Cui CZ, Tang DH, Zhang WT, Xin SG, et al. A molten-salt method to synthesize Co_9S_8 embedded, N, S co-doped mesoporous carbons from melamine formaldehyde resins for electrocatalytic hydrogen evolution reactions. Chempluschem. 2022;87(5):e202200077.
[73] Toro RG, Calandra P, Federici F, de Caro T, Mezzi A, Cortese B, et al. Development of superhydrophobic, self-cleaning, and flame-resistant DLC/TiO_2 melamine sponge for application in oil–water separation. J Mater Sci. 2020;55:2846–59.
[74] Wang HT, Meng XF, Qian ZZ, Zhou H, Ding YF, Zhang SM, et al. Synthesis and properties of melamine-formaldehyde/montmorillonite nanocomposites. J Nanosci Nanotechnol. 2008;8:1775–81.
[75] Hu X, Li MX, Yang J, Liu F, Huang H, Pan HF, et al. In situ fabrication of melamine hydroxy ethylidene diphosphonate wrapped montmorillonite for reducing the fire hazards of epoxy resin. Appl Clay Sci. 2021;201:105934.
[76] Jahromi AE, Jahromi HRE, Hemmati F, Saeb MR, Goodarzi V, Formela K. Morphology and mechanical properties of polyamide/

clay nanocomposites toughened with NBR/NBR-g-GMA: A comparative study. Compos Part B-Eng. 2016;90:478–84.
[77] Liang WD, Wang R, Wang CJ, Jia J, Sun HX, Zhang JL, et al. Facile preparation of attapulgite-based aerogels with excellent flame retardancy and better thermal insulation properties. J Appl Polym Sci. 2019;136(32).
[78] Liu S, Chevali VS, Xu ZG, Hui D, Wang H. A review of extending performance of epoxy resins using carbon nanomaterials. Compos Part B-Eng. 2018;136:197–214.
[79] Li HX, Jia DD, Ding MC, Zhou LJ, Wang K, Liu JQ, et al. Robust 3D graphene/cellulose nanocrystals hybrid lamella network for stable and highly efficient solar desalination. Sol RRL. 2021;5(8):2100317.
[80] Luo JM, Yang XQ, Tusiime R, Chen HN, Liu Y, Zhang H, et al. Synergistic effect of multiscale BNs/CNT and 3D melamine foam on the thermal conductive of epoxy resin. Compos Commun. 2022;29:101044.
[81] Shi HG, Wang T, Cheng JB, Zhao HB, Li SL, Wang YZ. Ultralow-density carbon foam composites with bean-like Co-embedded carbon nanotube whiskers towards high-performance microwave absorption. J Alloy Compd. 2021;863:158090.
[82] Jahankhah S, Sabzehmeidani MM, Ghaedi M, Dashtian K, Abbasi-Asl H. Hydrophilic magnetic molecularly imprinted resin in PVDF membrane for efficient selective removal of dye. J Environ Manag. 2021;300:113707.
[83] Rashid M, Islam MM, Minami H, Aftabuzzaman M, Rahman MA, Hossain MM, et al. Nickel decorated melamine-formaldehyde resin/polyaniline composites for high specific capacitance. Mater Chem Phys. 2020;249:122957.
[84] Xiong Z, Chen N, Wang Q. Preparation and properties of melamine formaldehyde resin modified by functionalized nano-SiO_2 and polyvinyl alcohol. Polym Polym Compos. 2021;29:96–106.
[85] Li CJ, Zhang HQ, Song YH, Cai LX, Wu JM, Wu JX, et al. Robust superhydrophobic and porous melamine-formaldehyde based composites for high-performance electromagnetic interference shielding. Colloids Surf A-Physicochem Eng Asp. 2021;624:126742.
[86] Schwarz D, Weber J. Organic-solvent free synthesis of mesoporous and narrow-dispersed melamine resin particles for water treatment applications. Polymer. 2018;155:83–8.
[87] Chen WM, Li S, Feizbakhshan M, Amdebrhan BT, Shi SK, Xin W, et al. TiO_2-SiO_2 nanocomposite aerogel loaded in melamine-impregnated paper for multi-functionalization: Formaldehyde degradation and smoke suppression. Constr Build Mater. 2018;161:381–8.
[88] Jalili MA, Khosroshahi Z, Kheirabadi NR, Karimzadeh F, Enayati MH. Green triboelectric nanogenerator based on waste polymers for electrophoretic deposition of titania nanoparticles. Nano Energy. 2021;90:106581.
[89] Liu KK, Su CQ, Ma WW, Li HL, Zeng Z, Li LQ. Free formaldehyde reduction in urea-formaldehyde resin adhesive: Modifier addition effect and physicochemical property characterization. Bioresources. 2020;15:2339–55.
[90] Xu WX, Dong SJ, Yu CH, Yan X, Xu JJ, Jiang MJ. Melamine formaldehyde/polyvinyl alcohol composite fiber: Structure and properties manipulated by hydroxymethylation degree. J Appl Polym Sci. 2014;131(17).
[91] Shi YQ, Shen JQ, Qiu T, Chu QD, Chen S, Ma M, et al. High impact strength modified melamine-formaldehyde resin with special "building blocks" structure. Polym Eng Sci. 2022;62:2165–75.
[92] Lulu L, Yongqiang K, Yangong Y, Rimin C, Zhao J. Structure and properties of melamine formaldehyde/polyvinyl alcohol (MF-PVA) composite fiber by electrospinning. Adv Mater Res (Switz). 2015;1088:419–23.
[93] Zhong BC, Gou WQ, Tang JL, Li QL, He Q. Constructing efficient and recyclable composite absorbent based on the modification of polymer skeleton with in situ assembled mesoporous silica/graphene oxide nanohybrid. Compos Sci Technol. 2022;220:109295.
[94] Wang Q, He L, Pan AZ, Wu YS. Removable/fluorescent adhesive made by melamine-formaldehyde cross-linked polyvinyl alcohol and its repair application in artifacts. Appl Surf Sci. 2019;495:143570.
[95] Zhu QM, Wang XH, Chen XQ, Yu CJ, Yin Q, Yan HQ, et al. Fabrication and evaluation of melamine-formaldehyde resin crosslinked PVA composite coating membranes with enhanced oxygen barrier properties for food packaging. RSC Adv. 2021;11:14295–305.
[96] Ti P, Liao YH, Wang QY, Qin ZJ, Cai QY, Lin Z, et al. Large-format preparation technology and electric heating performance of wooden electric heating flooring. Bioresources. 2022;17:4069–85.
[97] Fei XN, Zhao HB, Zhang BL, Cao LY, Yu MZ, Zhou JG, et al. Microencapsulation mechanism and size control of fragrance microcapsules with melamine resin shell. Colloids Surf A-Physicochem Eng Asp. 2015;469:300–6.
[98] Chen XY, Afreen S, Yu X, Dong CH, Kong QS. Modified melamine-formaldehyde resins improve tensile strength along with anti-fouling and flame retardancy in impregnation of cellulose paper. RSC Adv. 2019;9:36788–95.
[99] Konig A, Fehrenbacher U, Hirth T, Kroke E. Flexible polyurethane foam with the flame-retardant melamine. J Cell Plast. 2008;44:469–80.
[100] Zhang X, Wang K, Jiang H, Su Z, Yuan H. Preparation of light melamine formaldehyde foam. Plastics. 2015;44:14–7.
[101] Ruipeng SUN, Tieling JIN, Fuxiang CHU, Chunpeng W. Influence of formaldehyde/melamine ratio on properties of melmine-formaldehyde foam. Mod Chem Ind. 2011;31:32–5.
[102] Ma WL, Liu XY, Qiu ZR, Cai ZH, Diao JL, Huang Y. Hydrophobic and flame-retardant multifunctional foam for enhanced thermal insulation and broadband microwave absorption via a triple-continuous network of RGO/MWCNT-melamine composite. Carbon. 2022;196:913–22.
[103] Liao HH, Liu Y, Wang Q, Duan WF. Preparation and properties of a poly(vinyl alcohol) hydrogel-melamine formaldehyde foam composite. Polym Compos. 2019;40:2067–75.
[104] Si Q, Jin F, Yang J. Study on preparation of melamine-formaldehyde foam. N Chem Mater. 2017;45:125–7.
[105] Wan X, Liu D, Lang M. Preparation and properties of melamine-formaldehyde foam by microwave foaming. J Funct Polym. 2013;26:156–61.
[106] Li H, Sun J, Qian K. Study on the foaming process of rigid melamine foam. J Funct Mater. 2015;46:7131–4.
[107] Ma Y, Zhang W, Wang C, Xu Y, Li S, Chu F. Preparation and characterization of melamine modified urea-formaldehyde foam. Int Polym Process. 2013;28:188–98.
[108] Zhang YS, Duan HD, Wang XJ, Meng X, Qin DW. Preparation and properties of composites based on melamine-formaldehyde foam and nano-Fe_3O_4. J Appl Polym Sci. 2013;130:2688–97.

[109] Lei K, Sun Y, Xu H, Lang M. Preparation and performance characterization of tripolycyanamide formaldehyde resin foam modified by THIEC. J Funct Polym. 2016;29:329–34.
[110] Thongkham W, Lertsatitthanakorn C, Jitpukdee M, Jiramitmongkon K, Khanchaitit P, Liangruksa M. Conductive nanofilm/melamine foam hybrid thermoelectric as a thermal insulator generating electricity: Theoretical analysis and development. J Mater Sci. 2019;54:8187–201.
[111] Wang J, Yang WB, He FF, Xie CQ, Fan JH, Wu JY, et al. Superhydrophobic melamine-formaldehyde foam prepared by in-situ coprecipitation. Chem Lett. 2018;47:414–6.
[112] Wang Z, Zhang X, Xu Y, Chen G, Lin F, Ding H. Preparation and thermal properties of shape-stabilized composite phase change materials based on paraffin wax and carbon foam. Polymer. 2021;237:124361.
[113] Wang M, Chen YL, Qin YL, Wang TJ, Yang J, Xu F. Compressible, fatigue resistant, and pressure-sensitive carbon aerogels developed with a facile method for sensors and electrodes. ACS Sustain Chem Eng. 2019;7:12726–33.
[114] Wang K, Cheng ZF, Li PF, Zheng YW, Liu Z, Cui L, et al. Three-dimensional self-floating foam composite impregnated with porous carbon and polyaniline for solar steam generation. J Colloid Interface Sci. 2021;581:504–13.
[115] Meng S, Zhao X, Tang CY, Yu P, Bao RY, Liu ZY, et al. A bridge-arched and layer-structured hollow melamine foam/reduced graphene oxide composite with an enlarged evaporation area and superior thermal insulation for high-performance solar steam generation. J Mater Chem A. 2020;8:2701–11.
[116] Ye XL, Chen ZF, Ai SF, Hou B, Zhang JX, Zhou QB, et al. Effect of thickness of SiC films on compression and thermal properties of SiC/CF composites. Ceram Int. 2019;45:4674–9.
[117] Zhang JX, Chen ZF, Zhao W, Yang LX, Ye XL, Cui S, et al. Compressive behavior of the SiC-NWs/MCF composites with a designed double-nest microstructure. J Mater Sci. 2020;55:4170–8.
[118] Liu Y, Chen ZF, Zhang JX, Ai SF, Tang H. Ultralight and thermal insulation carbon foam/SiO_2 aerogel composites. J Porous Mater. 2019;26:1305–12.
[119] Zhang JX, Chen ZF, Ai SF, Ye XL, Guo SQ, Xue SH. Arisen Ni-Si compounds in the fabricated SiC-NWs/melamine-based carbon foam composites with ultralow thermal conductivty. Mater Res Express. 2019;6:065608.
[120] Huang B, Yue JL, Fan BH, Tang XZ, Liu Y, Huang XZ. Constructing hierarchical structure via in situ growth of CNT in SiO_2-coated carbon foam for high-performance EMI shielding application. Compos Sci Technol. 2022;222:109372.
[121] Wei B, Wang MQ, Yao ZJ, Chen ZP, Chen P, Tao XW, et al. Bimetallic nanoarrays embedded in three-dimensional carbon foam as lightweight and efficient microwave absorbers. Carbon. 2022;191:486–501.
[122] Lyu LF, Wang FL, Zhang X, Qiao J, Liu C, Liu JR. CuNi alloy/carbon foam nanohybrids as high-performance electromagnetic wave absorbers. Carbon. 2021;172:488–96.
[123] Jiang S, Qian K, Yu KJ, Zhou HF, Weng YX, Zhang ZW. Study on ultralight and flexible Fe_3O_4/melamine derived carbon foam composites for high-efficiency microwave absorption. Chem Phys Lett. 2021;779:138873.
[124] Li X-L, He Y-R, Qin Z-M, Chen M-J, Chen H-B. Facile fabrication, mechanical property and flame retardancy of aerogel composites based on alginate and melamine-formaldehyde. Polymer. 2019;181:121783.
[125] Jiang DG, Zhang JZ, Qin S, Hegh D, Usman KAS, Wang JF, et al. Scalable fabrication of $Ti_3C_2T_x$ MXene/RGO/carbon hybrid aerogel for organics absorption and energy conversion. ACS Appl Mater Interfaces. 2021;13:51333–42.
[126] Deng ZM, Tang PP, Wu XY, Zhang HB, Yu ZZ. Superelastic, ultralight, and conductive $Ti_3C_2T_x$ MXene/acidified carbon nanotube anisotropic aerogels for electromagnetic interference shielding. ACS Appl Mater Interfaces. 2021;13:20539–47.
[127] Xi SB, Wang LL, Xie HQ, Yu W. Solar-thermal energy conversion and storage of super black carbon reinforced melamine foam aerogel for shape-stable phase change composites. Int J Hydrogen Energy. 2022;47:12024–35.
[128] Wu KD, Cao JX, Qian Z, Luo Y, Niu B, Zhang YY, et al. Monolithic carbon aerogels within foam framework for high-temperature thermal insulation and organics absorption. J Colloid Interface Sci. 2022;618:259–69.
[129] Ye XL, Chen ZF, Ao SF, Hou B, Zhang JX, Liang XH, et al. Novel three-dimensional SiC/melamine-derived carbon foam reinforced SiO_2 aerogel composite with low dielectric loss and high impedance matching ratio. ACS Sustain Chem Eng. 2019;7:2774–83.
[130] Ye XL, Chen ZF, Ai SF, Hou B, Zhang JX, Zhou QB, et al. Enhanced electromagnetic absorption properties of novel 3D-CF/PyC modified by reticulated SiC coating. ACS Sustain Chem Eng. 2019;7:11386–95.
[131] Ye XL, Chen ZF, Li M, Wang T, Wu C, Zhang JX, et al. Microstructure and microwave absorption performance variation of SiC/C foam at different elevated-temperature heat treatment. ACS Sustain Chem Eng. 2019;7:18395–404.
[132] Ye XL, Chen ZF, Ai SF, Hou B, Zhang JX, Zhou QB, et al. Microstructure characterization and thermal performance of reticulated SiC skeleton reinforced silica aerogel composites. Compos Part B-Eng. 2019;177:107409.
[133] Ye XL, Chen ZF, Li M, Wang T, Zhang JX, Wu C, et al. Reticulated SiC coating reinforced carbon foam with tunable electromagnetic microwave absorption performance. Compos Part B-Eng. 2019;178:107479.
[134] Ye XL, Chen ZF, Zhang JX, Wu C, Zhou QB, Ai SF, et al. Double network nested foam composites with tunable electromagnetic wave absorption performances. Inorg Chem Front. 2019;6:1579–86.
[135] Ye XL, Chen ZF, Ai SF, Hou B, Zhang JX, Liang XH, et al. Synthesis and microwave absorption properties of novel reticulation SiC/Porous melamine-derived carbon foam. J Alloy Compd. 2019;791:883–91.
[136] Ye XL, Chen ZF, Ai SF, Hou B, Zhang JX, Zhou QB, et al. Effect of pyrolysis temperature on compression and thermal properties of melamine-derived carbon foam. J Anal Appl Pyrolysis. 2019;142:104619.
[137] Ye XL, Chen ZF, Ai SF, Hou B, Zhang JX, Liang XH, et al. Effects of SiC coating on microwave absorption of novel three-dimensional reticulated SiC/porous carbon foam. Ceram Int. 2019;45:8660–8.
[138] Ye XL, Chen ZF, Ai SF, Hou B, Zhang JX, Liang XH, et al. Porous SiC/melamine-derived carbon foam frameworks with excellent electromagnetic wave absorbing capacity. J Adv Ceram. 2019;8:479–88.
[139] Ye XL, Chen ZF, Ai SF, Zhang JX, Hou B, Zhou QB, et al. Mechanical and thermal properties of reticulated SiC aerogel composite prepared by template method. J Compos Mater. 2019;53:4117–24.

[140] Han T, Luo RY, Cui GY, Wang LY. Effect of SiC nanowires on the high-temperature microwave absorption properties of SiCf/SiC composites. J Eur Ceram Soc. 2019;39:1743–56.
[141] Liang CY, Wang ZJ. Eggplant-derived SiC aerogels with high-performance electromagnetic wave absorption and thermal insulation properties. Chem Eng J. 2019;373:598–605.
[142] Xiao SS, Mei H, Han DY, Dassios KG, Cheng LF. Ultralight lamellar amorphous carbon foam nanostructured by SiC nanowires for tunable electromagnetic wave absorption. Carbon. 2017;122:718–25.
[143] Jiang Y, Chen Y, Liu YJ, Sui GX. Lightweight spongy bone-like graphene@SiC aerogel composites for high-performance microwave absorption. Chem Eng J. 2018;337:522–31.
[144] Dong S, Hu P, Zhang XH, Han JC, Zhang YM, Luo XG. Carbon foams modified with in-situ formation of Si_3N_4 and SiC for enhanced electromagnetic microwave absorption property and thermostability. Ceram Int. 2018;44:7141–50.
[145] Yuan XY, Cheng LF, Zhang YJ, Guo SW, Zhang LT. Fe-doped SiC/SiO_2 composites with ordered inter-filled structure for effective high-temperature microwave attenuation. Mater Des. 2016;92:563–70.
[146] Yuan XY, Cheng LF, Zhang LT. Electromagnetic wave absorbing properties of SiC/SiO_2 composites with ordered inter-filled structure. J Alloy Compd. 2016;680:604–11.
[147] Zhong B, Sai TQ, Xia L, Yu YL, Wen GW. High-efficient production of SiC/SiO_2 core-shell nanowires for effective microwave absorption. Mater Des. 2017;121:185–93.
[148] Zhang XF, Zhao JQ, He X, Li QY, Ao CH, Xia T, et al. Mechanically robust and highly compressible electrochemical supercapacitors from nitrogen-doped carbon aerogels. Carbon. 2018;127:236–44.